STEADY-STATE MODIFIED REDFIELD SOLUTION FOR NONEQUILIBRIUM FERMIONIC SYSTEMS

XU XIANSONG

NATIONAL UNIVERSITY OF SINGAPORE

2016

STEADY-STATE MODIFIED REDFIELD SOLUTION FOR NONEQUILIBRIUM FERMIONIC SYSTEMS

XU XIANSONG

A THESIS SUBMITTED FOR THE DEGREE OF
BACHELOR OF SCIENCE

DEPARTMENT OF PHYSICS
NATIONAL UNIVERSITY OF SINGAPORE

2016

Declaration

I hereby declare that this thesis is my original work and it has been written by me in its entirety. I have duly acknowledged all the sources of information which have been used in the thesis.

This thesis has also not been submitted for any degree in any university previously.

Xu Xiansong

April 2016

朝闻道，夕死可矣。

——— *The Analects 4:8*

Acknowledgments

This thesis marks the end of my undergraduate study. However, the learning journey would never be ended. In this project, I would sincerely thank to a group of people. This thesis would never be possible without their consistent support and guidance.

Firstly, I would like to thank to my supervisor, Prof. Wang Jian-Sheng who brings into this field of study. His patient guidance is indispensable in the research life I have experienced. Both my undergraduate research project (UROPS) and my final year project would not be possible without him.

I would also like to express my gratitude to my collaborator, Dr. Juzar Thingna for consistent discussions and suggestions that help me go back on track whenever I am lost.

I am grateful for all the group members including: Mr. Ruofan Chen, Dr. Jianping Lu, Mr. Jiebin Peng, Mr. Hongfei Qiu, Dr. Jichang Ren, Mr. Han Hoe Yap, Ms. Li Zhang, and Dr. Hangbo Zhou, for fruitful discussions.

I would like to thank my friends Mr. Kunlun Dai, Mr. Baiyu Li, Mr. Yijiong Song, Mr. Senmao Tan, Mr. Zhuo Xu, and Mr. Hanwen Zhang for their kind help and support.

Last but not the least, I would like to thank my parents who support me all the way along. Without their efforts, I would not be able to make this far.

Abstract

Quantum master equation (QME) is an important concept for open quantum systems. Different types of quantum master equations are developed to described the non-unitary time evolution of systems that are coupled with environments. Due to the complexity of the generalized exact master equation, a possible simplification is to perform perturbative treatment. However, the perturbative treatment has limited ourselves into the weak coupling regime. In moderate or strong coupling regime, higher order master equations should be considered that have a high analytical and numerical complexity. One possible attempt to avoid such complexity is to perform analytic continuation techniques (AC) to the Redfield master equation (RME) and hence to obtain a modified Redfield solution (MRS) of the second order reduced density matrix (RDM). As compared to a common treatment that preserves a zeroth order accuracy to RDM, the modified Redfield solution so far gives exact results to second order RDM for quantum harmonic oscillator model and spin-boson model connected to bosonic baths. In this thesis, the modified Redfield solution is generalized to fermionic systems and the exactness of the solution is discussed. A comparison is also done against other types of master equations including the Redfield master equation and the Lindblad master equation (LME). The result gives an overall picture on how different master equation approaches behave in a varying coupling strength. The validity of using various master equations for transport problems is discussed.

Contents

List of Figures

List of Symbols and Abbreviations

List of Symbols

ρ	Reduced density matrix for system
ρ_{tot}	Total density matrix
Tr_B	Partial trace over the degrees of freedom of bath or environment
p_i	Probability of normalized state i
ψ_i	The wave function of state i for both the system and the bath
ϕ_i	The wave function of state i for the system only
H_{tot}	Hamiltonian of the total composite system including both the system, the bath and the system-bath coupling
H_S	Hamiltonian of the system of interest
H_B	Hamiltonian of the bath
V	System-bath coupling
λ	System-bath coupling strength
σ	Position of the bath
S	System operator
B	Bath operator
α, β	Types of system operator and bath operator
v	Tunnelling strength
t	Real time
$\mathcal{U}(t,0)$	Time evolution operator from time 0 to time t
$C(t)$	Bath correlator
Δ_{nm}	Energy spacing between energy level E_n and E_m
$\mathcal{R}$	Relaxation four tensor
W'	Transition rates, the real part of W
W''	Imaginary part of W

$\Gamma(\varepsilon)$	Spectral density
f_σ	Fermi-Dirac distribution
D	Two-point correlation matrix
G^+	Retarded Green's function
G^-	Advanced Green's function
Σ^+	Retarded self energy
Σ^-	Advanced self energy
g^+	Retarded surface Green's function
g^-	Advanced surface Green's function
h	Hopping energy
σ_z	Pauli matrix

List of Abbreviations

QME	Quantum master equation
AC	Analytic continuation
RME	Redfield master equation
RDM	Reduced density matrix
LME	Lindblad master equation
SQD	Single quantum dot
DQD	Double quantum dot
NEGF	Nonequilibrium Green's function
MRS	Modified Redfield solution
D.E.	Discrepancy error
h.c.	Hermitian conjugate
NESS	Nonequilibrium steady-state

Chapter 1

Introduction

The development of quantum mechanics in the last century has provided us a brand new perspective of the microscopic world. The studies on microscopic and mesoscopic phenomena would no longer be constrained in the classical regime and the quantum features of many phenomena are revealed. At an earlier stage, the elementary studies usually focus on isolated system in quantum mechanics as a natural generalization and correspondence of classical mechanics. However, the interaction between the system and the environment are overlooked for isolated systems while there does not exist an ideal isolated system in reality. Typical problems with contributions from the system-environment interaction lie in a wide range of topics in physics such as mesoscopic transport [8], quantum information [10], optics [4, 3], *etc.*. The system-environment interaction plays an indispensable role in such scenarios. This type of system is often known as an *open system* as a contrast to an *isolated system*. Particularly, when the system of interest is extremely small such that quantum mechanics plays an essential role, it is named as an *open quantum system* [2, 28, 20]. The environment is often called a bath or a reservoir and is considered equilibrated.

For an open quantum system, the energy and particle transfer capture the nonequilibrium features of such a system. These features can be captured via a *reduced density matrix* (RDM) [1] that can be viewed as a quantum counterpart of the classical phase space volume density. RDM is often defined by the taking the partial trace over the infinite degrees of freedom of the environment to the *total density matrix* that includes both the environment and the system of interest. It

naturally turns out that the key problem to be tackled in such a system is to find the RDM that contains all information of the system of interest. Therefore, the computation of the non-trivial nonequilibrium RDM is our primary target. Different approaches have been formulated to evaluate the RDM. The common approaches are grouped under an umbrella term known as quantum master equations. While the exact quantum master equation [17, 30] is often difficult to solve even with numerically exact approaches, perturbative treatments are often used in the weak system-bath coupling regime. It can be systematically extended to moderate coupling by taking into account higher order contributions [24, 11]. One commonly used perturbative master equation is the Redfield master equation (RME) [19] that resort to only the weak coupling approximation. Lindblad master equation (LME) [15, 7] is another widely used master equation that imposes an additional *secular approximation* to the RME. LME can also be formulated using quantum dynamical semi-group in a more mathematically rigorous way. LME is also known as the *Lindblad form* that is trace-preserving and preserves complete positivity. However, despite the long history that the RME has been formulated, the accuracy of RME has only been discussed in very recent years [6, 16]. It is found that the RME does not give an accurate result in steady state with a naive assumption that the second order density matrix solely depends on the second order relaxation tensor. To obtain the correct result up to second order, higher order relaxation tensor is required. Such higher order calculations are extremely tedious [24] and are difficult to be generalized. In order to circumvent these problems, the analytic continuation method (AC) [22, 23, 21] is proposed by J. Thingna *et al.* to obtain the RDM correct up to second order without calculating the higher order relaxation tensors. The AC method has been demonstrated on quantum harmonic oscillator and spin-boson model with bosonic baths. Thus, it would be interesting to investigate the validity of this method on fermionic systems.

In this thesis, by using the analytic continuation technique, a modified solution to the Redfield master equation is proposed for fermionic systems. Our approach

is demonstrated on spinless single quantum dot (SQD) model and spinless double quantum dot (DQD) models. We check the accuracy of the form of the second order RDM obtained via AC for fermionic systems against the nonequilibrium green's function (NEGF) method [5, 27, 9]. The results are also compared with RME and LME. Such comparison would provide an overall picture on the adequacy of determination by using various master equations.

This thesis is structured in the following way. In chapter 2, an introduction to reduced density matrix formalism used in open quantum system is given. For quantum master equation approaches, we present a microscopic derivation of Redfield master equation and Lindblad master equation. The nonequilibrium Green's function approach is briefly discussed. In the end, we present an accuracy comparison scheme. In chapter 3, the accuracy issue with RME is discussed and the modified Redfield solution is obtained for fermionic system via the analytic continuation technique. In chapter 4, we propose a single quantum dot model and two types of double quantum dot models to examine the exactness of the modified Redfield solution using the comparison scheme introduced in chapter 2. The exactness is checked against NEGF. In chapter 5, the modified Redfield solution is compared against other master equations including RME and LME. In the end, we present the conclusion in chapter 6.

THIS PAGE IS INTENTIONALLY LEFT BLANK

Chapter 2

Reduced Density Matrix Formalism

2.1 Overview

The quantum master equation could be in general regarded as a first order differential equation that describes the time evolution of the reduced density matrix. The probabilistic nature originates from the physical stochastic processes possessed by the system of interest due to the inaccessibility to the complete knowledge of the environment.

Classically, master equations could appear in the forms of Boltzmann equation, Fokker-Planck equation, *etc.*. Such master equations give a complete description of the probability density function that defines the property of the system.

In quantum mechanics, the probability density function concept in phase space is replaced by the reduced density matrix. For open quantum system, the total density matrix would be describing both the environment and the system. Moreover, the bath as an environment should be an infinite bath to maintain equilibrium which has infinitely many of degrees of freedom that makes the problem unsolvable. The RDM is obtained by coarse graining (tracing out) over the infinite degree of freedom of the environment. The equation governing the evolution of such a RDM is known as a quantum master equation in the theory of open quantum systems. QME help retain the crucial bath information of the environment without increasing the complexity beyond the system Hilbert space.

In 1928, Pauli has given the first quantum master equation known as the Pauli

master equation or rate equation [18] that is used to describe the occupation number in weak coupling. Redfield in 1957 developed a master equation [19] that describes the environment-spin interaction for nuclear magnetic resonance. The Nakajima−Zwanzig master equation is formulated by Nakajima in 1958 [17] and by Zwanzig in 1960 [30]. It is also known as the generalized master equation that preserves a form of integro-differential equation. In 1976, Gorini, Kossakowski, and Sudarshan proposed an alternative QME [7] by using quantum dynamical semigroup formalism for finite dimensional Hilbert space. In the same year, Lindblad provided a deep mathematical understanding [15] to the structure of this QME and showed that it preserves positivity. In general, all the perturbative second order master equation can be obtained from the RME by imposing appropriate approximations. For example, the Lindblad master equation is obtained by imposing the secular approximation on the Redfield master equation. In the case of the Pauli master equation, only the diagonal elements are taken into account.

In this chapter, a general introduction to density matrix and the reduced density matrix is given. A general setup for open quantum system is formulated. We then present a microscopic derivation of the RME. Based on the derivation for RME, the LME with an additional secular approximation (also known as rotating wave approximation) is formulated and we compare it with the quantum dynamical semigroup formalism for the Lindblad form.

2.1.1 Reduced Density Matrix

The density matrix formulation [14, 26] developed in 1928 generalized the description of quantum mechanics from the wave function based description of isolated systems to open systems. For open quantum system, the system of interest is always coupled with the bath. The total density matrix for the bath and the system that form a composite isolated system seems to be able to obtain in standard treatment for closed systems. However, the size of the bath is considered

as infinitely large and the total density matrix would essentially not be a suitable quantity to study the system of interest. Therefore, the degrees of freedom of the bath have to be coarse-grained over. The resultant form is the reduced density matrix defined as

$$\rho \;=\; \mathrm{Tr}_B\left(\rho_{tot}\right). \tag{2.1}$$

This trace-taking process is known as the partial trace over the infinite degrees of freedom of the environment or the bath. The total density matrix ρ_{tot} is a composite form for the system of interest, the baths, and the system-bath interactions.

Such total density matrix ρ_{tot} can be defined as

$$\rho_{tot} \;=\; \sum_i p_i \left|\psi_i\right\rangle \left\langle\psi_i\right|, \tag{2.2}$$

where p_i is the probability of the normalized state $|\psi_i\rangle$ that belongs to the total Hilbert space including both the system and the bath. The sum $\sum_i p_i = 1$ and $|\psi_i\rangle$ is in the Hilbert space of the system of interest. In general, the state $|\psi_i\rangle$ does not need to be orthogonal. RDM yields a similar definition except that it will be defined by the normalized state $|\phi_i\rangle$ that belongs to the Hilbert space of the system only.

The key properties of the RDM can be summarized into the following points:

1. Hermicity: $\rho^\dagger = \rho$.
2. Normalization: $\mathrm{Tr}_S\left(\rho\right) = 1$.
3. Positivity: $\left\langle\phi_i\right| \rho \left|\phi_i\right\rangle \geq 0$.
4. Purity : $\mathrm{Tr}_S\left(\rho^2\right) \leq 1$.

Hermicity is required for common quantum mechanics operator. Normalization and positivity arise due to the probabilistic nature of the density matrix. The

last property give us a good indication for the purity of state. In general, pure state will give us $\mathrm{Tr}_S\left(\rho^2\right) = 1$ and mixed states would give us $\mathrm{Tr}_S\left(\rho^2\right) < 1$.

It is necessary to clarify that in many other contexts the above mentioned density matrix is often named as *density operator* and the matrix form of the density operator is then regarded as density matrix in different representation.

What we really concerns is the system of interest, the observable of the system would be defined by $\langle A\rangle = \mathrm{Tr}_S\left(\rho\hat{A}\right)$ that is solely related to the RDM. The observable of the composite system can be calculated from the density matrix $\langle A\rangle = \mathrm{Tr}\left(\rho_{tot}\hat{A}\right)$. However, since the bath is usually considered as infinitely large, such observable would often be meaningless to discuss. For example, the energy and the number of particles of the composite system would be infinitely large.

2.1.2 Generic Setup for Open Quantum System

For an open quantum system, the total Hamiltonian reads

$$H_{tot} \quad = \quad H_S + H_B + \lambda V, \tag{2.3}$$

where H_S is the Hamiltonian for the system of our interest, H_B is the bath Hamiltonian. V is system-bath coupling Hamiltonian with λ denoting the coupling strength.

The bath Hamiltonian H_B is often regarded as infinitely large. The bath could be describe as an equilibrium distribution characterized by a fixed temperature T and a fixed chemical potential μ. The bath can be chosen to suit different requirements in transport problems. For example, the bath can be chosen as an electronic bath or harmonic oscillator bath. The coupling term can often be cast into a general form

$$V = \sum_{\sigma} V_\sigma = \sum_{\sigma} \sum_{i,\alpha=1,2} S_i^\alpha \otimes B_{i\sigma}^\alpha, \tag{2.4}$$

where α indicates the type of system operator and σ indicates the position of the baths with respect to the system of interest. The baths Hamiltonian would then have the form $H_B = \sum_\sigma H_\sigma$.

For example, for a single quantum dot coupled with two baths, we have

$$\begin{aligned} S^1 &= d, && (2.5)\\ S^2 &= d^\dagger, && (2.6)\\ B^1_\sigma &= \sum_{k\sigma} v_{k\sigma} c^\dagger_{k\sigma}, && (2.7)\\ B^2_\sigma &= \sum_{k\sigma} v^*_{k\sigma} c_{k\sigma}, && (2.8) \end{aligned}$$

and the form of coupling writes $V = V_L + V_R = \sum_{kL} v_{kL} d c^\dagger_{kL} + \sum_{kR} v_{kR} d c^\dagger_{kR} + \text{h.c.}$ with v as the tunnelling strength.

2.2 Quantum Master Equation Approach

2.2.1 Redfield Master Equation

Given the total Hamiltonian as Eq. (2.3), the time evolution of the total density matrix is given by

$$\rho_{tot}(t) = \mathcal{U}(t,0)\,\rho_{tot}(0)\,\mathcal{U}^\dagger(t,0). \quad (2.9)$$

The time evolution operator then takes the form

$$\begin{aligned} \mathcal{U}(t,0) &= e^{-iH_{tot}t} \\ &= e^{-i(H_0+\lambda V)t}, && (2.10) \end{aligned}$$

with $H_0 = H_S + H_B$. Throughout this thesis, $\hbar$ and k_B are set equal to 1.

Obtaining the total density matrix Eq. (2.9) exactly is a cumbersome task due to the presence of system-bath coupling term V. In order to make the problem

tractable, we use the Kubo identity given by Eq. (2.11) [See Appendix A for detailed proof] to perturbatively expand over the coupling as shown below.

The Kubo identity [13] has the following expression

$$e^{\nu\left(\hat{A}+\hat{B}\right)} = e^{\nu\hat{A}}\left[\mathbb{1}+\int_0^{\nu} d\tau e^{-\tau\hat{A}}\hat{B}e^{\tau\left(\hat{A}+\hat{B}\right)}\right], \tag{2.11}$$

By identifying

$$\hat{B} = -i\lambda V, \tag{2.12}$$

$$\hat{A} = -iH_0, \tag{2.13}$$

$$\nu = t, \tag{2.14}$$

the time evolution operator of the total density matrix has the form

$$\mathcal{U}(t,0) = \mathcal{U}_0(t,0)\left[\mathbb{1}-i\lambda\int_0^t d\tau\mathcal{U}_0^{\dagger}(\tau,0)\,V\mathcal{U}(\tau,0)\right], \tag{2.15}$$

with $\mathcal{U}_0(t,0)=e^{-iH_0t}$.

By substituting $\mathcal{U}(t,0)$ recursively into above equation and keeping the terms up to second order coupling, the time evolution operator can be written as

$$\begin{aligned} & \mathcal{U}(t,0) \\ \approx\ & \mathcal{U}_0(t,0)\left[\mathbb{1}-i\lambda\int_0^t d\tau V(\tau)-\lambda^2\int_0^t\int_0^{\tau} d\tau d\tau' V(\tau)\,V\left(\tau'\right)\right] \\ =\ & \mathcal{U}_0(t,0)\,\mathcal{U}_I(t,0), \end{aligned} \tag{2.16}$$

where

$$V(\tau) = \mathcal{U}_0^{\dagger}(\tau,0)\,V\mathcal{U}_0(\tau,0), \tag{2.17}$$

$$\mathcal{U}_I(t,0) = \mathbb{1}-i\lambda\int_0^t d\tau V(\tau)-\lambda^2\int_0^t\int_0^{\tau} d\tau d\tau' V(\tau)\,V\left(\tau'\right). \tag{2.18}$$

Eq. (2.9) depicts the time evolution of density matrix in Schroedinger picture

where as Eq. (2.17) represents the time evolution of operator in interaction picture. The term $\mathcal{U}_I(t,0)$ represents the effect on the time evolution of total system due to of system-bath coupling. By doing so, the final form of RDM could be maintained in Schroedinger picture. An alternative derivation that works in interaction picture for the RDM can be referred to [2].

Now we consider the time evolution of the total density matrix $\dot{\rho}_{tot}(t) = d\left(\mathcal{U}(t,0)\,\rho_{tot}(0)\,\mathcal{U}^{\dagger}(t,0)\right)/dt$, by applying the perturbative time evolution operator Eq. (2.16). Thus, in the *weak* system-bath coupling regime, we obtain

$$\begin{aligned}\dot{\rho}_{tot}(t) &= -i\left[H_0, \rho_{tot}(t)\right] - i\lambda\left[V, \tilde{\rho}_{tot}(t)\right] \\ &\quad +\lambda^2 \int_0^t d\tau \left[V, \left[\tilde{\rho}_{tot}(t), V(\tau - t)\right]\right], \end{aligned} \tag{2.19}$$

with $\tilde{\rho}_{tot}(t) = e^{iH_0 t}\rho_{tot}(t)\,e^{-iH_0 t}$ known as the evolution of the total density matrix in the interaction picture.

However, we are interested in the reduced density matrix which is ρ. This could be done by performing partial trace with respect to the bath degrees of freedom

$$\begin{aligned}\mathrm{Tr}_B\left[\dot{\rho}_{tot}(t)\right] &= \frac{d}{dt}\mathrm{Tr}_B\left[\rho_{tot}(t)\right] \\ &= \frac{d}{dt}\rho(t). \end{aligned} \tag{2.20}$$

During the trace-taking process, we have assumed $\langle B\rangle_B = 0$. The immediate consequence would be that $\mathrm{Tr}_B\left(\left[V, \tilde{\rho}_{tot}(t)\right]\right) = 0$ as $\mathrm{Tr}_B\left(B\rho_B(t)\right) = 0$. We take the liberty to have such a assumption due to the fact that a nonzero $\langle B\rangle_B$ would only provide an energy shift to the total Hamiltonian. A new system-bath coupling can be defined by $V = S \otimes (B - \langle B\rangle_B)$. This assumption is known as *centering of baths*.

Together with the *decoupled initial condition* that $\rho_{tot}(0) = \rho(0) \otimes \rho_B(0)$ and

Born approximation that $\rho_B(0) \approx \rho_B(t)$ one can find that

$$\begin{aligned}\frac{d\rho(t)}{dt} &= -i\left[H_S, \rho(t)\right] \\ &\quad -\sum_{\sigma\alpha\beta}\int_0^t d\tau \left\{\left[S^\alpha, \tilde{S}^\beta(\tau - t)\,\tilde{\rho}(t)\right] C_\sigma^{\alpha\beta}(t-\tau) + \text{h.c.}\right\}, \quad (2.21)\end{aligned}$$

where $C^{\alpha\beta}(t)$ is the bath correlation function defined as $\left\langle \tilde{B}^\alpha(t)\, B^\beta(0)\right\rangle$. The coupling strength term is absorbed in the spectral density of the bath correlation.

The decoupled initial condition assumes that the system-bath coupling is only turned on at time $t = 0$. Such condition would provide us a time reference that we can start to take account the effect of system-bath coupling. It is not a strict condition as it is always possible to manipulate the system or the bath such that no system-bath coupling exist at a point of time. The Born approximation assumes that the bath is always relaxed as the relaxation time of the bath is always much shorter than the time evolution scale due to the bath's infinite size and its pre-assumed equilibrium condition.

A further approximation is made that $\tilde{\rho}(t) \approx \rho(t)$ due to the weak coupling condition. This allow us to rewrite Eq. (2.21) as

$$\begin{aligned}\frac{d\rho(t)}{dt} &= -i\left[H_S, \rho(t)\right] \\ &\quad -\sum_{\sigma\alpha\beta}\int_0^t d\tau \left\{\left[S^\alpha, \tilde{S}^\beta(\tau - t)\,\rho(t)\right] C_\sigma^{\alpha\beta}(t-\tau) + \text{h.c.}\right\}. \quad (2.22)\end{aligned}$$

The above equation is known as the Redfield master equation [19]. The first term describes the free evolution of the Hamiltonian and the second term describes the dissipative features of bath on the system due to system-bath interaction.

In the energy eigenbasis of the system, the above equation can be rewritten as

$$\frac{d}{dt}\rho_{nm} = -i\Delta_{nm}\rho_{nm} + \sum_{i,j}\mathcal{R}_{nm}^{ij}\rho_{ij}, \quad (2.23)$$

where $\Delta_{ij} = E_i - E_j$ with E_i denoting the ith eigenenergy of the system and

$\mathcal{R}^{ij}_{nm}$ known as the *relaxation tensor*

$$\begin{aligned}\mathcal{R}^{ij}_{nm} &= \sum_{\sigma}\sum_{\alpha\beta} S^{\alpha}_{ni}S^{\beta}_{jm}\left(W^{\alpha\beta}_{\sigma ni}+W^{\alpha\beta *}_{\sigma mj}\right) \\ &\quad -\delta_{m,j}\sum_{l} S^{\alpha}_{nl}S^{\beta}_{li}W^{\alpha\beta}_{\sigma li}-\delta_{i,n}\sum_{l} S^{\alpha}_{jl}S^{\beta}_{lm}W^{\alpha\beta *}_{\sigma lj}. \end{aligned} \tag{2.24}$$

Above W is defined as

$$W^{\alpha\beta}_{\sigma ij} = \int_0^t d\tau e^{-i\Delta_{ij}\tau}C^{\alpha\beta}_{\sigma}(\tau), \tag{2.25}$$

with the real part of W known as the *transition rate*.

We denote

$$W^{'\alpha\beta}_{\sigma ij} = \mathrm{Re}\left(W^{\alpha\beta}_{\sigma ij}\right), \tag{2.26}$$

$$W^{''\alpha\beta}_{\sigma ij} = \mathrm{Im}\left(W^{\alpha\beta}_{\sigma ij}\right). \tag{2.27}$$

The function $\Gamma(\varepsilon)$ is the spectral density. The detailed calculation of W and the bath correlators can be referred to Appendix B where we assumed electronic baths with a Lorentzian spectral density. The evaluation the transition rate $W^{'\alpha\beta}_{\sigma ij}$ would allow us to obtain an important condition which is known as the *detailed balance condition* for *fermionic systems*

$$\frac{W'^{21}_{\sigma ij}}{W'^{12}_{\sigma ij}} = \frac{f_{\sigma}(\varepsilon, T_{\sigma}, \mu_{\sigma})}{1-f_{\sigma}(\varepsilon, T_{\sigma}, \mu_{\sigma})}, \tag{2.28}$$

with

$$W'^{12}_{\sigma ij} = \frac{1}{2}\Gamma_{\sigma ij}(\varepsilon) f_{\sigma}(\varepsilon, T_{\sigma}, \mu_{\sigma}), \tag{2.29}$$

$$W'^{21}_{\sigma ij} = \frac{1}{2}\Gamma_{\sigma ij}(\varepsilon)\Big[1-f_{\sigma}(\varepsilon, T_{\sigma}, \mu_{\sigma})\Big]. \tag{2.30}$$

The detailed balance condition describes the equilibration of a process due to its

reversed process occurred for equilibrium bath in steady-state.

In steady state limit, that is, if we assume the system will reach steady state after evolving for a sufficient long time, the reduced density matrix would no longer be time dependent in the limit $t \to \infty$. Hence, we claim that $d\rho/dt = 0$ in steady state and Eq. (2.25) can be rewritten as

$$W_{ij}^{\alpha\beta} = \int_{-\infty}^{t} d\tau e^{-i\Delta_{ij}(t-\tau)} C^{\alpha\beta}(t-\tau), \tag{2.31}$$

such that the system-bath coupling is switched on at $-\infty$ and a steady state is reached at t.

With the condition that $d\rho/dt = 0$, we would be able to solve the RME as a linear algebra problem. As mentioned in the introduction, the solution of the RME provides a solution that is accurate up to zeroth order. A detailed explanation would be presented in the next chapter.

2.2.2 Lindblad Master Equation

The other well-known master equation is known as Lindblad master equation [15] (also known as Gorini-Kossakowski-Sudarshan-Lindblad equation [7]). The LME can be formulated by using quantum dynamical semigroup. The dynamical map to the reduced density matrix from the its initial state and a fixed state preserves the semigroup property. The final form of generator of the dynamical semigroup is usually known as the Lindbald form or the LME. By adopting the quantum dynamical semigroup formalism, the trace-preserving property and complete positivity can be easily viewed. However, despite the fact that the formalism is mathematically rigorous, such form does not provide us with a clear physical picture. A more physically friendly yet not so general approach can be achieved by performing secular approximation to the RME. A general method by performing secular approximation is given in [2], we reproduce its derivation and show that it is equivalent with the Lindblad form in the Appendix. An

alternative approach [29] could be done by considering a rotating frame.

In the rotating frame, the density matrix $\tilde{\rho}_{nm}(t) = \rho_{nm}e^{-i\Delta_{nm}t}$. The RME followed from Eq. (2.23) in its energy eigenbasis could be represented as

$$\frac{d}{dt}\tilde{\rho}_{nm} = \sum_{ij}\mathcal{R}^{ij}_{nm}\tilde{\rho}_{ij}e^{i(\Delta_{nm}-\Delta_{ij})t}. \tag{2.32}$$

The secular approximation requires all the terms $e^{i(\Delta_{nm}-\Delta_{ij})t}$ with $\Delta_{nm} \neq \Delta_{ij}$ averaging to zero. As such, only $\Delta_{nm} = \Delta_{ij}$ remains and the Lindblad form could be represented as

$$\frac{d\rho_{nn}}{dt} = \sum_{i}\mathcal{R}^{ii}_{nn}\rho_{ii}, \tag{2.33}$$

$$\frac{d\rho_{nm}}{dt} = -i\Delta_{nm}\rho_{nm} + \mathcal{R}^{nm}_{nm}\rho_{nm}, \tag{2.34}$$

with R^{nm}_{nm} only contains the real parts of the transition rates.

The term $(\Delta_{nm} - \Delta_{ij})^{-1}$ with $\Delta_{nm} \neq \Delta_{ij}$ defines the time scale τ_S for the intrinsic evolution of the system which is large as compared to the system's relaxation time τ_R. Hence the terms $e^{i(\Delta_{nm}-\Delta_{ij})t}$ are highly oscillating during the time scale on ρ.

However, the above forms would be not so clear to give a direct connection to the Lindblad form below. We shown in Appendix C an alternative way which has a clearer connection to the Lindblad form.

The Lindblad Form obtained by quantum dynamical semigroup [2, 15, 7] is given as

$$\frac{d\rho}{dt} = \mathcal{L}\rho = -i\left[H,\rho\right] + \sum_{k=1}^{N^2-1}\gamma_k\left(A_k\rho A_k^\dagger - \frac{1}{2}A_k^\dagger A_k\rho - \frac{1}{2}\rho A_k^\dagger A_k\right). \tag{2.35}$$

2.3 Nonequilibrium Green's Function Approach

Nonequilibrium Green's function approach is another powerful tool in dealing with nonequilibrium many-particle problems. NEGF is also formulated to calculate the RDM [5]. The RDM formalism for fermionic system using NEGF is briefly discussed below.

We still adopt the Hamiltonian for the generic setup introduced in Eq. (2.3).

The steady-state two point-correlation matrix is defined as

$$\begin{aligned} D_{ij} &= \left\langle d_i^\dagger d_j \right\rangle_S \\ &= \mathrm{Tr}_S \left(\rho d_i^\dagger d_j \right) \\ &= \mathrm{Tr} \left(\rho_{tot} d_i^\dagger d_j \right). \end{aligned} \tag{2.36}$$

For a quadratic Hamiltonian, the correlation matrix D can be calculated exactly. By representing the correction matrix using the following Green's functions

$$G^\pm = \frac{1}{\varepsilon - H_s - \sum_\sigma \Sigma_\sigma^\pm(\varepsilon)}. \tag{2.37}$$

The correlation matrix D can be cast into the form

$$\begin{aligned} D_{ij} &= \left\langle d_i^\dagger d_j \right\rangle_S \\ &= \frac{1}{2\pi} \int_{-\infty}^{\infty} d\varepsilon \sum_\sigma \left[\left(G^+ \Gamma_\sigma(\varepsilon) G^- \right)_{ji} f_\sigma(\varepsilon, T_\sigma, \mu_\sigma) \right], \end{aligned} \tag{2.38}$$

where f_σ is the Fermi-Dirac distribution $\left[e^{\beta_\sigma(\varepsilon - \mu_\sigma)} + 1 \right]^{-1}$ with $\beta_\sigma = T_\sigma^{-1}$.

$\Sigma_\sigma^\pm(\varepsilon)$ are known as the retarded (+) or advanced (-) self-energies of the bath at σ and is given by

$$\Sigma_\sigma^\pm(\varepsilon) = V_\sigma g_\sigma^\pm V_\sigma^\dagger, \tag{2.39}$$

where $g_\sigma^\pm$ are the surface Green's function of the baths given by $g_\sigma^\pm(\varepsilon) =$

$[\varepsilon \pm i\eta - H_\sigma]^{-1}$.

$\Gamma_\sigma(\varepsilon)$ known as the spectral density of the bath at σ and is defined by

$$\Gamma_\sigma(\varepsilon) = i\left(\Sigma_\sigma^+ - \Sigma_\sigma^-\right). \tag{2.40}$$

Due to the system-bath coupling, this matrix would possess off-diagonal elements and we could define a new sets of fermionic operators by diagonalizing the D. The diagonal elements of the new diagonalized matrix Λ as λ_i. The transformation reads $U^\dagger DU = \Lambda$. The new operator would then take the form

$$d'_s = \sum_l U_{ls} d_l. \tag{2.41}$$

Recall the form of a fermionic occupation number with energy ε_i

$$n(\varepsilon_i) = \frac{\exp(-\beta\varepsilon_i)}{\prod_i^N [1+\exp(-\beta\varepsilon_i)]}. \tag{2.42}$$

We could write down an effective Fermi-Dirac distribution for each fermions s

$$\rho = \prod_{s=1}^{N} \frac{\exp\left(-a_s d_s'^\dagger d'_s\right)}{[1+\exp(-a_s)]}, \tag{2.43}$$

with $a_s = \ln\left(\lambda_s^{-1} - 1\right)$ obtained via $\left\langle d_s'^\dagger d'_s \right\rangle = \lambda_s = [\exp(a_s)+1]^{-1}$.

2.4 Comparison Scheme

Nonequilibrium Green's function approach provides us with the exact solution to the reduced density matrix. To check the accuracy of the solution from perturbative quantum master equation, we impose a comparison scheme by checking the discrepancy error.

We formally expand the RDMs obtained via NEGF and the QME as

$$\rho_{NEGF} = \sum_{n=0} \lambda^{2n} \rho^{(2n)}_{NEGF}\,, \tag{2.44}$$

$$\rho_{QME} = \sum_{n=0} \lambda^{2n} \rho^{(2n)}_{QME}\,. \tag{2.45}$$

The discrepancy error is then given by

$$\text{D.E.}^{(i)} = \frac{\rho_{NEGF} - \rho_{QME}}{\lambda^i}, \tag{2.46}$$

where i is the order of accuracy we want to check against.

Suppose we want to check if the QME is accuracy up to zeroth order, we find that the

$$\begin{aligned} \text{D.E.}^{(0)} &= \rho_{NEGF} - \rho_{QME} \\ &= \sum_{n=0} \lambda^{2n} \Delta\rho^{(2n)} \\ &= \Delta\rho^{(0)} + \lambda^2 \Delta\rho^{(2)} + \lambda^4 \Delta\rho^{(4)} + \cdots\,, \end{aligned} \tag{2.47}$$

where $\Delta\rho^{(2n)} = \rho^{(2n)}_{NEGF} - \rho^{(2n)}_{QME}$. If $\rho^{(0)}_{QME}$ is accurate, $\Delta\rho^{(0)} = 0$ and D.E. would be at the order of λ^2. The discrepancy error would converge to 0 in the limit $\lambda \to 0$.

Similarly suppose we want to check if QME is accuracy up to 2nd order,

$$\begin{aligned} \text{D.E.}^{(2)} &= \frac{\rho_{NEGF} - \rho_{QME}}{\lambda^2} \\ &= \sum_{n=0} \lambda^{2n-2} \Delta\rho^{(2n)} \\ &= \frac{\Delta\rho^{(0)}}{\lambda^2} + \Delta\rho^{(2)} + \lambda^2 \Delta\rho^{(4)} + \cdots\,. \end{aligned} \tag{2.48}$$

If ρ_{QME} is accurate up to second order, $\Delta\rho^{(0)} = \Delta\rho^{(2)} = 0$ and D.E. is again in the order of λ^2. We could again check the limit of the discrepancy error when λ approaches 0 and if the results match up to second order, the $\text{D.E.}^{(2)} \to 0$ as

$\lambda \to 0$.

In chapter 4, we used D.E.$^{(2)}$ to check the second order RDM. For the zeroth order RDM, an analytical proof is obtained for SQD using the weak coupling approximation via NEGF and QME. A numerical comparison is done by using the weak coupling approximation for DQD models.

Chapter 3

Modified Redfield Solution

3.1 Modified Solution of Redfield Master Equation

Two most commonly used master equations are introduced in the previous chapter. In the chapter, the accuracy of the Redfield master equation is discussed in the first part, which serves as the motivation for analytic continuation method. In the second part, the AC method is constructed for fermionic system as a generalization of the method that had been demonstrated on systems with bosonic baths in previous publications [22, 23].

3.1.1 Accuracy of Redfield Master Equation

Intuitively, it may be easily assumed that by solving a second-order equation, the density matrix solved would be accurate up to second order. However, C.H. Fleming and N.I. Cummings [6] have shown that this is not the case. In general, to obtain the solutions of accuracy of order-$2n$, the master equation of order-$(2n+2)$ is required. For RME, a typical perturbative second order master equation, would only provide a solution that is accurate at zeroth order as a $n = 1$ case.

We consider a generic perturbation series expansion to all orders in the formally exact master equation

$$\frac{\partial \rho}{\partial t} = \left(\overline{\Delta} + \sum_{n=1}^{\infty} \lambda^{2n} R^{(2n)} \right) \rho. \tag{3.1}$$

If we rearrange the ρ into a column vector with its diagonal part and off-diagonal part separated in the form of $\begin{pmatrix} \rho_d \\ \\ \rho_{od} \end{pmatrix}$, we can also express $\overline{\Delta}$ as $\begin{pmatrix} 0 & 0 \\ \\ 0 & \overline{\Delta}_{22} \end{pmatrix}$ and the four tensor $\mathcal{R}^{(2n)}$ as $\begin{pmatrix} R_{nn}^{ii(2n)} & R_{nn}^{ij,i\neq j(2n)} \\ \\ R_{nm,n\neq m}^{ii(2n)} & R_{nm,n\neq m}^{ij,i\neq j(2n)} \end{pmatrix}$. We reassign the index and use 1 to denote $i = j$ or $n = m$ and 2 to denote $i \neq j$ or $n \neq m$. The first index refers to the relation between n and m and the second index refers to the relation between i and j. The four tensor $\mathcal{R}^{(2n)}$ can be then represented as $\begin{pmatrix} R_{11}^{(2n)} & R_{12}^{(2n)} \\ \\ R_{21}^{(2n)} & R_{22}^{(2n)} \end{pmatrix}$.

By doing so, we could obtain

$$\frac{\partial}{\partial t}\begin{pmatrix} \rho_d \\ \\ \rho_{od} \end{pmatrix} = \left[\begin{pmatrix} 0 & 0 \\ \\ 0 & \overline{\Delta}_{22} \end{pmatrix} + \left(\sum_{n=1}^{\infty} \lambda^{2n} R^{(2n)}\right)\right]\begin{pmatrix} \rho_d \\ \\ \rho_{od} \end{pmatrix}. \tag{3.2}$$

In the long time limit $t \to \infty$, the system would evolve to steady state such that we can apply the steady state condition $\partial\rho/\partial t = 0$. The time dependence in the four tensor can be dropped in the long time limit since the steady state is reached.

By formally expanding the RDM, we have

$$\rho \;=\; \sum_{n=0}^{\infty} \lambda^{2n} \rho^{(2n)}. \tag{3.3}$$

Hence, a master equation that contains all orders of RDM is obtained in steady-

state

$$\left[\begin{pmatrix} 0 & 0 \\ 0 & \overline{\Delta}_{22} \end{pmatrix} + \left(\sum_{n=1}^{\infty} \lambda^{2n} R^{(2n)}\right)\right]\left[\sum_{n=0}^{\infty} \lambda^{2n} \begin{pmatrix} \rho_d^{(2n)} \\ \rho_{od}^{(2n)} \end{pmatrix}\right] = 0. \tag{3.4}$$

An order-by-order check can be performed to analyze the dependence of $\rho^{(2n)}$ on the relaxation tensor $\mathcal{R}^{(2n)}$. We demonstrate the accuracy issue for RME which is a second order QME. In general, such check can be expanded to arbitrary order.

For the zeroth order case when $n = 0$

$$\begin{pmatrix} 0 & 0 \\ 0 & \overline{\Delta}_{22} \end{pmatrix} \lambda^0 \begin{pmatrix} \rho_d^{(0)} \\ \rho_{od}^{(0)} \end{pmatrix} = 0. \tag{3.5}$$

We can compare the coefficient of λ^0 and obtain

$$\rho_{od}^{(0)} \;=\; 0. \tag{3.6}$$

This indicates that the off-diagonal element of the zeroth density matrix should always be zero.

For the second order case when $n = 1$, we have

$$\left[\begin{pmatrix} 0 & 0 \\ 0 & \overline{\Delta}_{22} \end{pmatrix} + \left(\lambda^2 R^{(2)}\right)\right]\left[\lambda^0 \begin{pmatrix} \rho_d^{(0)} \\ \rho_{od}^{(0)} \end{pmatrix} + \lambda^2 \begin{pmatrix} \rho_d^{(2)} \\ \rho_{od}^{(2)} \end{pmatrix}\right] = 0. \tag{3.7}$$

We require the coefficient of λ^2 to be 0. Together with the condition $\rho_{od}^{(0)} = 0$, we

have

$$R_{11}^{(2)}\rho_d^{(0)} = 0, \tag{3.8}$$

$$\overline{\Delta}_{22}\rho_{od}^{(2)} + R_{21}^{(2)}\rho_d^{(0)} = 0. \tag{3.9}$$

Above equations imply that $\rho_d^{(0)}$ is dependent on second order $\mathcal{R}^{(2)}$ only and $\rho_{od}^{(2)}$ relies on $\rho_d^{(0)}$ and $\mathcal{R}^{(2)}$.

A similar procedure applies to fourth order λ^4 and we obtain

$$R_{11}^{(2)}\rho_d^{(2)} + R_{12}^{(2)}\rho_{od}^{(2)} + R_{11}^{(4)}\rho_d^{(0)} = 0, \tag{3.10}$$

$$\overline{\Delta}_{22}\rho_{od}^{(4)} + R_{21}^{(2)}\rho_d^{(2)} + R_{22}^{(2)}\rho_{od}^{(2)} + R_{21}^{(4)}\rho_d^{(0)} = 0. \tag{3.11}$$

Again we see that $\rho_d^{(2)}$ and $\rho_{od}^{(4)}$ requires $\mathcal{R}^{(4)}$ to be fully determined.

In a more compact way, the dependence of the reduced density matrix on relaxation tensors is given by:

$$\rho^{(0)} \rightarrow \left\{R^{(2)}\right\}, \tag{3.12}$$

$$\rho_{od}^{(2)} \rightarrow \left\{R^{(2)}\right\}, \tag{3.13}$$

$$\rho_d^{(2)} \rightarrow \left\{R^{(2)}, R^{(4)}\right\}, \tag{3.14}$$

$$\rho_{od}^{(4)} \rightarrow \left\{R^{(2)}, R^{(4)}\right\}. \tag{3.15}$$

It can be observed that to obtain the second order off-diagonal elements, we need the zeroth order and the second order relaxation tensor. To obtain the second order diagonal elements we need to know the 4th order relaxation tensor from equation. The RME is a second order QME which does not contain any information for $\mathcal{R}^{(4)}$. Hence the accuracy of the solution provide by RME would only be accurate up to full zeroth order RDM and off-diagonal second order RDM. A more general proof can be referred to [6] which shows explicitly that to determine $\rho^{(2n)}$ correctly, $\mathcal{R}^{(2n+2)}$ is required.

This accuracy issue brought out an important aspect on the validity of using of RME as it is only accurate to zeroth order. And we know that zeroth order RDM would be the result obtained at $\lambda = 0$ if we consider Eq. (3.3). The second order RDM correction term would not even be accurate in the weak coupling regime.

To obtain a correct correction term at second order, fourth order relaxation tensor need to be calculated that is tedious to achieve. A possible approach by performing analytic continuation technique to $\rho_{od}^{(2)}$ is formulated by J. Thingna *et al.* The resultant modified Redfield solution has matched exactly for second order RDM for harmonic oscillator and spin-boson model connected to bosonic bath. The information of the exactness on fermionic systems with fermionic bats is unknown. In the next part, we formulate the modified Redfield solution using analytic continuation techniques for fermionic system based on previous formalism for bosonic baths.

3.1.2 Analytic Continuation Method

In the previous section, the dependence on the density matrix and the relaxation tensor is revealed. The problem that whether it is possible to obtain the second order density matrix by avoiding the higher order relaxation tensor calculation has emerged. It turns out that this is indeed possible by obtaining the diagonal elements of the second order density matrix from the off-diagonal elements of the second order density matrix.

In chapter 2, the RME in its eigenbasis has been found

$$\frac{d\rho_{nm}}{dt} = -i\Delta_{nm}\rho_{nm} + \sum_{i,j}\mathcal{R}_{nm}^{ij}\rho_{ij}, \tag{3.16}$$

where we omit the index for position σ in $W_{\sigma ij}^{\alpha\beta}$ in this chapter. Hence the

relaxation four tensor is given by

$$\begin{aligned}\mathcal{R}^{ij}_{nm} &= \sum_{\sigma}\sum_{\alpha\beta} S^{\alpha}_{ni}S^{\beta}_{jm}\left(W^{\alpha\beta}_{ni}+W^{\alpha\beta *}_{mj}\right) \\ &\quad -\delta_{m,j}\sum_{l} S^{\alpha}_{nl}S^{\beta}_{li}W^{\alpha\beta}_{li}-\delta_{i,n}\sum_{l} S^{\alpha}_{jl}S^{\beta}_{lm}W^{\alpha\beta *}_{lj}. \end{aligned} \tag{3.17}$$

In the previous section, we obtain the dependence of the zeroth order RDM in Eq. (3.6) and Eq. (3.8). In the eigenbasis representation

$$\rho^{(0)}_{ij}=0, \tag{3.18}$$

$$\sum_{\sigma,i,\alpha\beta}\left[W^{\alpha\beta}_{ni}S^{\alpha}_{ni}S^{\beta}_{in}-\delta_{n,i}\sum_{l}W^{\alpha\beta}_{li}S^{\alpha}_{nl}S^{\beta}_{li}\right]\rho^{(0)}_{ii}=0. \tag{3.19}$$

Similarly, the dependence of the second order off-diagonal RDM in Eq. (3.9) can be represented as

$$\rho^{(2)}_{nm}=i\sum_{\sigma,i,\alpha\beta}\frac{S^{\alpha}_{ni}S^{\beta}_{im}}{\Delta_{nm}}\left[\left(W^{\alpha\beta}_{im}\rho^{(0)}_{mm}+W^{\alpha\beta *}_{in}\rho^{(0)}_{nn}\right)-\left(W^{\alpha\beta}_{ni}+W^{\alpha\beta *}_{mi}\right)\rho^{(0)}_{ii}\right]. \tag{3.20}$$

If we treat $\rho^{(2)}_{nm}$ as a function of Δ_{nm} and let Δ_{nm} be extremely small such $\rho^{(2)}_{nm}\to\rho^{(2)}_{nn}$, it can be found that

$$\rho^{(2)}_{nn} = i\sum_{\sigma,i,\alpha\beta}\frac{S^{\alpha}_{ni}S^{\beta}_{in}}{\Delta_{nn}}\left[W'^{\alpha\beta}{}_{in}\rho^{(0)}_{nn}-W'^{\alpha\beta}{}_{ni}\rho^{(0)}_{ii}\right], \tag{3.21}$$

which preserve a $0/0$ indeterminate form as $R^{(2)}_{11}\rho^{(0)}_{d}=0$.

In a more compact notation, when we are taking $n=m$, it is equivalent to have

$$\rho^{(2)}_{od} = \frac{-R^{(2)}_{11}\rho^{(0)}_{d}}{\overline{\Delta}_{12}}. \tag{3.22}$$

However, that does not imply that a limiting value of $\lim_{m\to n}\rho_{nm}$ with appropriate choice of a path does not exist.

If we take $E_m \to E_n - z$, we have

$$\begin{aligned}
\rho_{nn}^{(2)} &= \lim_{z\to 0} i \sum_{\sigma,i,\alpha\beta} \frac{S_{ni}^{\alpha} S_{in}^{\beta}}{E_n - (E_n - z)} \Big[\left(W_{in}^{\alpha\beta}(z)\, \rho_{mm}^{(0)} + W_{in}^{\alpha\beta *}(0)\, \rho_{nn}^{(0)} \right) \\
&\quad - \left(W_{ni}^{\alpha\beta}(0) + W_{ni}^{\alpha\beta *}(-z) \right) \rho_{ii}^{(0)} \Big] \\
&= \lim_{z\to 0} i \sum_{\sigma,i,\alpha\beta} \frac{S_{ni}^{\alpha} S_{in}^{\beta}}{z} \Big[\left(W_{in}^{'\alpha\beta}(z)\, \rho_{nn}^{(0)} + W_{in}^{'\alpha\beta}(0)\, \rho_{nn}^{(0)} \right) \\
&\quad - \left(W_{ni}^{'\alpha\beta}(0) + W_{ni}^{'\alpha\beta}(-z) \right) \rho_{ii}^{(0)} \Big] \\
&\quad - \lim_{z\to 0} \sum_{\sigma,i,\alpha\beta} \frac{S_{ni}^{\alpha} S_{in}^{\beta}}{z} \Bigg[\left(W_{in}^{''\alpha\beta}(z)\, \rho_{nn}^{(0)} + W_{in}^{''\alpha\beta}(0)\, \rho_{nn}^{(0)} \right) \\
&\quad + W_{in}^{''\alpha\beta}(z)\, z \frac{\partial \rho_{nn}^{(0)}}{\partial E_n} - \left(W_{ni}^{'\alpha\beta}(0) + W_{ni}^{''\alpha\beta}(-z) \right) \rho_{ii}^{(0)} \Bigg], \qquad (3.23)
\end{aligned}$$

where we have expanded $\rho_{nn}^{(0)}(z)$ in the following way

$$\rho_{nn}^{(0)}(z) = \rho_{nn}^{(0)} + z \frac{\partial \rho_{nn}^{(0)}}{\partial E_n}. \qquad (3.24)$$

We have assumed

$$\frac{\partial \rho_{nn}^{(0)}}{\partial E_i} = 0 \text{ for } i \neq n. \qquad (3.25)$$

In the chapter 4 Sec. 4.3, we claim that this is a valid assumption.

In the limit $z \to 0$, $W'(z) = W'(-z) = W'(0) = W'$, with V_{ni}'' defined as

$\partial W''_{ni}/\partial\Delta_{ni}$, the previous equation reads

$$\begin{aligned}
\rho^{(2)}_{nn} &= \lim_{z\to 0} i \sum_{\sigma,i,\alpha\beta} \frac{S^{\alpha}_{ni}S^{\beta}_{in}}{z}\Big[\left(W'^{\alpha\beta}_{in}(z)\,\rho^{(0)}_{nn} + W'^{\alpha\beta}_{in}(0)\,\rho^{(0)}_{nn}\right) \\
&\quad - \left(W'^{\alpha\beta}_{ni}(0) + W'^{\alpha\beta}_{ni}(-z)\right)\rho^{(0)}_{ii}\Big] \\
&\quad - \lim_{z\to 0}\sum_{\sigma,i,\alpha\beta} \frac{S^{\alpha}_{ni}S^{\beta}_{in}}{z}\Bigg[\left(W''^{\alpha\beta}_{in}(z)\,\rho^{(0)}_{nn} + W''^{\alpha\beta}_{in}(0)\,\rho^{(0)}_{nn}\right) \\
&\quad + W''^{\alpha\beta}_{in}(z)\, z\frac{\partial\rho^{(0)}_{nn}}{\partial E_n} - \left(W''^{\alpha\beta}_{ni}(0) + W''^{\alpha\beta}_{ni}(-z)\right)\rho^{(0)}_{ii}\Bigg] \\
&= \lim_{z\to 0}\sum_{\sigma,i,\alpha\beta} S^{\alpha}_{ni}S^{\beta}_{in}\Bigg[\left(\frac{W''^{\alpha\beta}_{in}(0) - W''^{\alpha\beta}_{in}(-z)}{-z}\right)\rho^{(0)}_{nn} \\
&\quad - W''^{\alpha\beta}_{in}(z)\frac{\partial\rho^{(0)}_{nn}}{\partial E_n} + \left(\frac{W''^{\alpha\beta}_{ni}(0) - W''^{\alpha\beta}_{ni}(-z)}{-z}\right)\rho^{(0)}_{ii}\Bigg] + \bar{\rho}^{(2)}_{nn} \\
&= \sum_{\sigma,i,\alpha\beta} S^{\alpha}_{ni}S^{\beta}_{in}\left[\left(-V''^{\alpha\beta}_{in}\rho^{(0)}_{nn} + V''^{\alpha\beta}_{ni}\rho^{(0)}_{ii}\right) + W''^{\alpha\beta}_{in}\frac{\partial\rho^{(0)}_{nn}}{\partial E_n}\right]. \qquad (3.26)
\end{aligned}$$

In the last step, the term $\bar{\rho}^{(2)}_{nn}$ is dropped as we find that

$$\begin{aligned}
\bar{\rho}^{(2)}_{nn} &= \lim_{z\to 0} i \sum_{\sigma,i,\alpha\beta} \frac{S^{\alpha}_{ni}S^{\beta}_{in}}{z}\Big[\left(W'^{\alpha\beta}_{in}(z)\,\rho^{(0)}_{nn} + W'^{\alpha\beta}_{in}(0)\,\rho^{(0)}_{nn}\right) \\
&\quad - \left(W'^{\alpha\beta}_{ni}(0) + W'^{\alpha\beta}_{ni}(-z)\right)\rho^{(0)}_{ii}\Big] \\
&= 0. \qquad (3.27)
\end{aligned}$$

Hence, the diagonal component of the density matrix can be thus represented as

$$\rho^{(2)}_{nn} = \sum_{\sigma,i,\alpha\beta} S^{\alpha}_{ni}S^{\beta}_{in}\left[\left(-V''^{\alpha\beta}_{in}\rho^{(0)}_{nn} + V''^{\alpha\beta}_{ni}\rho^{(0)}_{ii}\right) + W''^{\alpha\beta}_{in}\frac{\partial\rho^{(0)}_{nn}}{\partial E_n}\right]. \qquad (3.28)$$

The term $\partial\rho^{(0)}_{nn}\Big/\partial E_n$ can be determined via the Eq. (3.8), $R^{(2)}_{11}\rho^{(0)}_{d} = 0$, by taking partial derivatives E_i to both side. The result takes the form

$$\frac{\partial\rho^{(0)}_{nn}}{\partial E_n} = \frac{\sum_{\sigma,i\neq n,\alpha\beta} S^{\alpha}_{ni}S^{\beta}_{in}\left(V^{\alpha\beta(0)}_{ni}\rho^{(0)}_{ii} + V^{\alpha\beta}_{in}\rho^{(0)}_{nn}\right)}{\sum_{\sigma,i\neq n,\alpha\beta} W'^{\alpha\beta}_{in}S^{\alpha}_{ni}S^{\beta}_{in}}. \qquad (3.29)$$

To normalize the RDM at second order, we consider the following normalization condition

$$\begin{aligned}\rho_{nn} &= \frac{\rho_{nn}^{(0)}+\rho_{nn}^{(2)}}{\sum_i\left(\rho_{ii}^{(0)}+\rho_{ii}^{(2)}\right)} \\ &\approx \left(\rho_{nn}^{(0)}+\rho_{nn}^{(2)}\right)\left(1-\sum_i \rho_{ii}^{(2)}\right) \\ &\approx \rho_{nn}^{(0)}+\rho_{nn}^{(2)}-\rho_{nn}^{(0)}\sum_i \rho_{ii}^{(2)}. \end{aligned} \tag{3.30}$$

By applying the normalization condition $\sum_n \rho_{nn}=1$ and $\sum_n \rho_{nn}^{(0)}=1$, we sum up the above equation and it gives

$$1 = 1+\sum_n\left(\rho_{nn}^{(2)}-\rho_{nn}^{(0)}\sum_i \rho_{ii}^{(2)}\right). \tag{3.31}$$

Hence the normalized $\rho_{nn}^{(2)}$ takes the final form

$$\begin{aligned}\rho_{nn}^{(2)} &= \sum_{\sigma,i,\alpha\beta} S_{ni}^{\alpha}S_{in}^{\beta}\left[\left(-V_{in}^{''\alpha\beta}\rho_{nn}^{(0)}+V_{ni}^{''\alpha\beta}\rho_{ii}^{(0)}\right)+W_{in}^{''\alpha\beta}\frac{\partial\rho_{nn}^{(0)}}{\partial E_n}\right] \\ &\quad -\rho_{nn}^{(0)}\sum_{\sigma,i,\alpha\beta} S_{ij}^{\alpha}S_{ji}^{\beta}W_{ji}^{''\alpha\beta}\frac{\partial\rho_{ii}^{(0)}}{\partial E_i}, \end{aligned} \tag{3.32}$$

with Eq. (3.31) implying its traceless property.

This is the final form obtained using the analytic continuation method. The resultant RDM with second order correction $\rho_{MRS}=\rho^{(0)}+\lambda^2\rho^{(2)}$ is known as the *modified Redfield solution*.

In summary, to obtain the MRS, we first solve zeroth order RDM $\rho^{(0)}$ via Eq. (3.8) or more explicitly by Eq. (3.18) and Eq. (3.19). The second order off-diagonal RDM $\rho_{od}^{(2)}$ would be supplied by Eq. (3.20). The normalized second order diagonal RDM is then calculated via the analytic continuation result in Eq. (3.32).

THIS PAGE IS INTENTIONALLY LEFT BLANK

Chapter 4

Exactness of the Modified Redfield Solution

The modified Redfield solution has been demonstrated on quantum harmonic oscillator and spin-boson model with bosonic baths [22, 21]. The results are shown to be exact by applying the comparison scheme. In this chapter, by performing the analytic continuation technique for fermionic systems, we would like to check whether such exactness still preserves.

Quantum dot [12] is a suitable fermionic system of interest. It is an artificial nanostructure that can confine electrons. Experimentally, two different types of dots could be structured. Vertical dots could be structured with high spatial symmetry . Lateral dot could be constructed by using metallic gates in a plane that has lower spatial symmetry. We are interested in how does the quantum dot serves as an open system and interact with the bath. For electronic baths, we would be able to study the electron transport properties. One interesting effect would be the Coulomb blockade effect that allows us to adjust the number of electrons in the quantum dot due to the Coulomb repulsion between electrons on the quantum dot.

For exactness check, we consider a spinless single quantum dot model and two types of double quantum dots model [25].

4.1 Spinless Single Quantum Dot

Hamiltonian

Consider a SQD coupled with two baths, the total Hamiltonian can be written as

$$H_{tot} = H_S + H_L + H_R + V_L + V_R, \tag{4.1}$$

with

$$\begin{aligned} H_S &= \varepsilon_0 d^\dagger d, && (4.2)\\ H_L &= \sum_{kL} \varepsilon_{kL} c_{kL}^\dagger c_{kL}, && (4.3)\\ H_R &= \sum_{kR} \varepsilon_{kR} c_{kR}^\dagger c_{kR}, && (4.4)\\ V_L &= \sum_{kL} v_{kL} d c_{kL}^\dagger + \text{h.c.}, && (4.5)\\ V_R &= \sum_{kR} v_{kR} d c_{kR}^\dagger + \text{h.c.}. && (4.6) \end{aligned}$$

$d^\dagger$ and d are the creation and annihilation operator for electrons representing excitation and de-excitation of an electron respectively. ε_0 represents the on-site energy level of the dot and ε_{kL} and ε_{kR} are the dispersion relations of the baths. k refers to the momentum index. The bath Hamiltonian is assumed to be solvable such that it can be written in above diagonal form in momentum space. v represents the tunnelling strength.

The SQD can be described using the schematic picture in Fig 4.1. A single quantum dot is coupled to two electronic baths. The baths are assumed to be in respective equilibrium and hence it can be well described by Fermi distributions that are defined by temperature T_σ and chemical potential μ_σ.

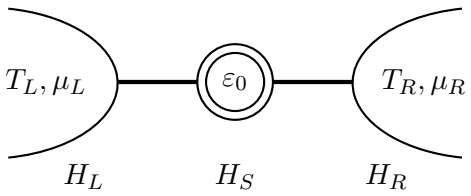

Figure 4.1: A schematic figure of a single quantum dot. A single quantum dot with on-site energy ε_0 coupled with two fermionic baths in respective equilibrium with fixed temperature T_σ and chemical potential μ_σ

Master Equation of a Sinlge Quantum Dot

With the above Hamiltonian, by using the recipe introduced in chapter 2, we would be able to write down the explicit form of the RME in energy eigenbasis as

$$\begin{aligned}\frac{d\rho_{nm}}{dt} &= -i\Delta_{nm}\rho_{nm}(t) \\ &+ \sum_{\sigma=L,R}\sum_{ij}\Big[S^2_{ni}S^1_{jm}W^{21*}_{mj\sigma} + S^2_{ni}S^1_{jm}W^{21}_{ni\sigma} \\ &-\delta_{m,j}\sum_l S^2_{nl}S^1_{li}W^{12}_{li\sigma} - \delta_{i,n}\sum_l S^2_{jl}S^1_{lm}W^{12*}_{lj\sigma} \\ &+S^1_{ni}S^2_{jm}W^{12}_{ni\sigma} + S^1_{ni}S^2_{jm}W^{12*}_{mj\sigma} \\ &-\delta_{i,n}\sum_l S^1_{jl}S^2_{lm}W^{21*}_{lj\sigma} - \delta_{m,j}\sum_l S^1_{nl}S^2_{li}W^{21}_{li\sigma}\Big]\rho_{ij}, \end{aligned} \tag{4.7}$$

where S^2 and S^1 are system operator $d^\dagger$ and d respectively in energy eigenbasis. For SQD, the Fock basis $|00\rangle$,$|01\rangle$, $|10\rangle$,$|11\rangle$ are equivalent to the energy eigenbasis since the system is only one-levelled. We have the liberty to express

$$S^1 = d = \begin{pmatrix} 0 & 1 \\ & \\ 0 & 0 \end{pmatrix}, \tag{4.8}$$

$$S^2 = d^\dagger = \begin{pmatrix} 0 & 0 \\ & \\ 1 & 0 \end{pmatrix}. \tag{4.9}$$

Directly solving Eq. (4.7) would give us the standard Redfield solution to the

RDM. To obtain the modified Redfield solution, we follow the treatment described in chapter 3 by using the relaxation tensor defined in Eq. (4.7) to obtain $\rho^{(0)}$ and $\rho^{(2)}_{od}$. $\rho^{(2)}_{d}$ is then calculated via the AC analytic result in Eq. (3.32). The LME can also be obtained via secular approximation on Eq. (4.7).

Nonequilibrium Green's Function for Single Quantum Dot

To obtain the exact RDM, the nonequilibrium Green's function approach for RDM formalism is used. The retarded Green's function of SQD is given by

$$G^{+}(\varepsilon) = \frac{1}{\varepsilon - \varepsilon_0 - \Sigma_L^{+}(\varepsilon) - \Sigma_R^{+}(\varepsilon)}, \tag{4.10}$$

with the self-energy given in Appendix E.

The correlation matrix D can be written as

$$\begin{aligned}\left\langle d^{\dagger} d \right\rangle = & \int_{-\infty}^{+\infty} d\varepsilon \frac{1}{2\pi} \left| G^{+}(\varepsilon) \right|^2 \Big[\Gamma_L(\varepsilon) f_L(\varepsilon, T_L, \mu_L) \\ & + \Gamma_R(\varepsilon) f_R(\varepsilon, T_R, \mu_R) \Big],\end{aligned} \tag{4.11}$$

that is a number for SQD system due to the size of the system.

The density matrix would then take the form

$$\rho = \frac{\exp\left(-a c_0^{\dagger} c_0\right)}{1 + \exp(-a)}, \tag{4.12}$$

with

$$a = \ln\left(D^{-1} - 1\right). \tag{4.13}$$

It can be found that

$$\rho = \begin{pmatrix} 1-D & 0 \\ 0 & D \end{pmatrix}. \tag{4.14}$$

4.1.1 Weak Coupling Limit Discussion

In weak coupling limit such that $\lambda \to 0$, we expect that the MRS would give us $\rho^{(0)}$ since the MRS is in the form $\rho^{(0)} + \lambda^2 \rho^{(2)}$. We known in chapter 3 that $\rho^{(0)}$ can be obtained via solving $R_{11}^{(2)} \rho^{(0)} = 0$

$$\begin{aligned} \sum_{\sigma=L,R} \Big[& 2S^2_{ni} S^1_{in} W'^{21}_{ni\sigma} - 2\delta_{n,i} \sum_l S^2_{nl} S^1_{li} W'^{12}_{li\sigma} \\ & + 2S^1_{ni} S^2_{in} W'^{12}_{ni\sigma} - 2\delta_{i,n} \sum_l S^1_{il} S^2_{ln} W'^{21}_{li\sigma} \Big] \rho_{ii} = 0. \end{aligned} \tag{4.15}$$

The above form reduces to the following equation if we consider the non-zero elements for system operator in its matrix representation $S^1_{12} = 1$ and $S^2_{21} = 1$:

$$\begin{bmatrix} W'^{12}_{21\sigma} & -W'^{21}_{12\sigma} \\ W'^{21}_{21\sigma} & -W'^{12}_{12\sigma} \end{bmatrix} \begin{bmatrix} \rho^{(0)}_{11} \\ \rho^{(0)}_{22} \end{bmatrix} = 0, \tag{4.16}$$

$$\left(\Gamma_L f_L + \Gamma_R f_R\right) \rho^{(0)}_{11} - \left(\Gamma_L \left(1 - f_L\right) + \Gamma_R \left(1 - f_R\right)\right) \rho^{(0)}_{22} = 0. \tag{4.17}$$

Together with the normalization condition that $\sum_i \rho^{(0)}_{ii} = 1$, we have

$$\rho^{(0)}_{11} = 1 - \frac{\Gamma_L f_L + \Gamma_R f_R}{\Gamma_L + \Gamma_R}. \tag{4.18}$$

This is exactly the form if we perform weak coupling approximation to NEGF for SQD.

For NEGF, the weak coupling limit implies Σ_L^+ and $\Sigma_R^+ \to 0$. The Green's function Eq. (4.10) would be effectively given by

$$G^+(\varepsilon) = \frac{1}{\varepsilon - \varepsilon_0 - i\frac{1}{2}(\Gamma_L + \Gamma_R)}. \tag{4.19}$$

The correlation matrix would take the form

$$\begin{aligned}\left\langle d^\dagger d \right\rangle &= \int_{-\infty}^{+\infty} d\varepsilon \frac{1}{2\pi} \frac{1}{(\varepsilon - \varepsilon_0)^2 + \frac{1}{4}(\Gamma_L(\varepsilon) + \Gamma_R(\varepsilon))^2} \Big[\Gamma_L(\varepsilon) f_L(\varepsilon, T_L, \mu_L) \\ &\quad + \Gamma_R(\varepsilon) f_R(\varepsilon, T_R, \mu_R)\Big].\end{aligned} \tag{4.20}$$

By using the identity

$$\lim_{\epsilon \to 0} \frac{\epsilon}{(x-a)^2 + \epsilon^2} = \pi \delta(x-a), \tag{4.21}$$

we have

$$D = \left\langle d^\dagger d \right\rangle = \frac{\Gamma_L f_L + \Gamma_R f_R}{\Gamma_L + \Gamma_R}. \tag{4.22}$$

Eq. (4.14) would then provide a form for ρ_{11}

$$\begin{aligned}\rho_{11} &= 1 - D \\ &= 1 - \frac{\Gamma_L f_L + \Gamma_R f_R}{\Gamma_L + \Gamma_R},\end{aligned} \tag{4.23}$$

which is exactly the same as compared to the zeroth order RDM result obtained via master equation given by Eq. (4.18). This implies that by checking the result for NEGF in the weak coupling limit, the zeroth order RDM result can be recovered.

The zeroth order RDM results have been shown to be analytically equal. A more general form of the weak coupling limit result can be referred to [5]. We then proceed to investigate the exactness of second order RDM.

4.1.2 Exactness Check in Equilibrium

In equilibrium situation where both the left bath and the right bath preserve the same temperature and same chemical potential, the system is effectively coupled with one bath and hence there would be not net currents flow through the dot.

We adopt the comparison scheme proposed in chapter 2 and compare the second order RDM obtained via AC and NEGF. The discrepancy error of interest would be D.E.$^{(2)}$ as had been argued in chapter 2. When the coupling strength $\lambda \to 0$, the D.E.$^{(2)}$ should also approach to 0 which is reflected by the y-intercept of the fitted line for D.E.$^{(2)}$ versus λ^2. By choosing a pair of equilibrium parameters, the D.E.$^{(2)}$ versus coupling strength λ^2 figure is given in Fig. 4.2

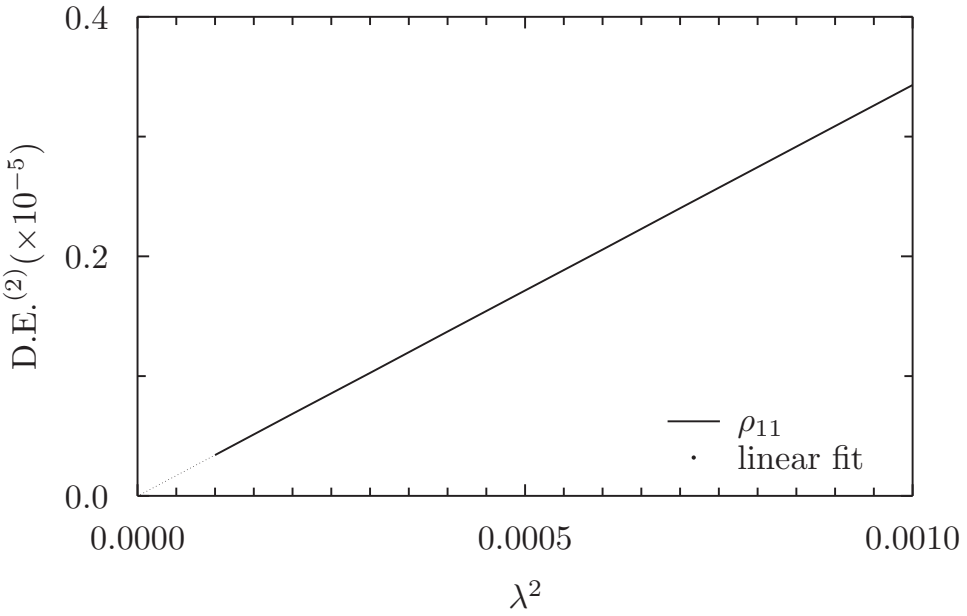

Figure 4.2: Figure of discrepancy error for ground state population ρ_{11} versus the coupling strength λ^2; $T_L = T_R = 0.25$ and $\mu_L = \mu_R = 0$. The cut-off energy ε_D is 1. The coupling strength is chosen from 0.0001 to 0.001. The y-intercept is given by -2.1534×10^{-8} which indicates a good match between $\rho^{(2)}_{MRS}$ and $\rho^{(2)}_{NEGF}$,

For a single quantum dot, the dimension of the Hilbert space is 2 and the RDM only have two diagonal elements. Hence, we take the liberty to check only of the diagonal element namely ρ_{11} as ρ_{22} is simply given by $1-\rho_{22}$ due to normalization condition of RDM.

The y-intercept is at the order 10^{-8} which is a good indication that the second order RDM of MRS is exact. We are not able to obtain a solution at machine precision of 10^{-15} due to the calculation of W. The calculation involves summing over all the Matsubara frequencies that is impossible as there are infinite many of terms. Certain convergence criterion is required. Throughout the thesis, the convergence criterion for the Matsubara sum is set to 10^{-15}. However, this does not indicate that our solution is accurate to 10^{-15}. Depending on the number of terms that are summed up, the error can add up to 10^{-9} if 10^{6} terms are summed up. Hence 10^{-8} would be a good indication that our determination of the exactness of second order RDM for MRS. For previous the work [22] done for bosonic baths in equilibrium, an analytic proof is given for the equivalence of the second order RDM in equilibrium.

4.1.3 Exactness Check in Nonequilibrium Steady-state

In the previous case, the exactness of second order RDM for MRS has been checked. We have argued that by performing a linear fitting, the y-intercept with a value of order 10^{-8} is a valid indication of the exactness of the second order RDM for MRS. We check if this is true in nonequilibrium steady-state. In NESS, the system of interest is connected to baths with different chemical temperatures and/or different chemical potentials. The discrepancy error plot in nonequilibrium is given by Fig. 4.3.

By performing linear fitting, a similar conclusion can be drawn as compared to equilibrium situation as the y-intercept is again at the order 10^{-8}. This allows us to conclude that the MRS is exact up to second order in nonequilibrium steady-state for single quantum dot system.

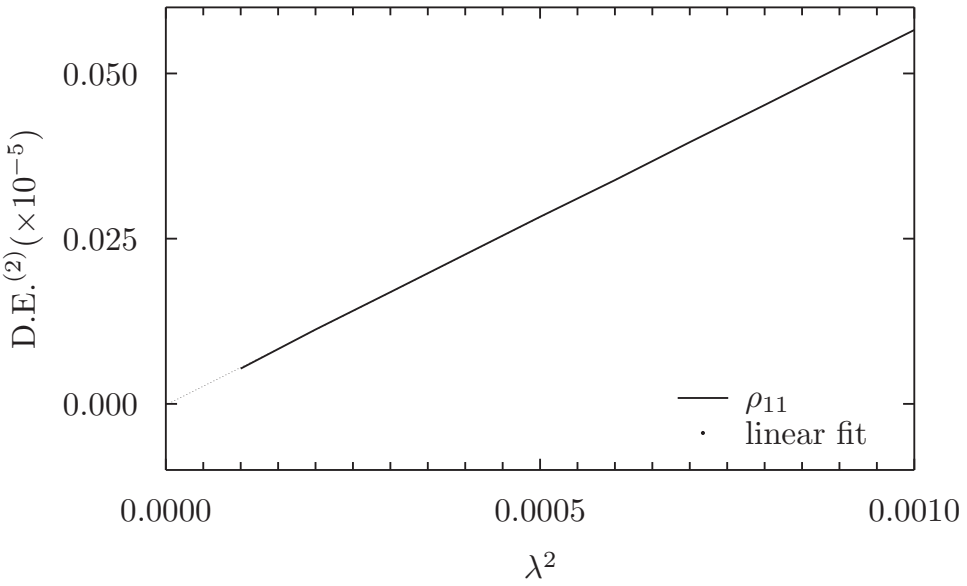

Figure 4.3: Figure of discrepancy error for ground state population versus the coupling strength λ^2; $T_L = 0.50$, $T_R = 0.25$ and $\mu_L = 1$, $\mu_R = 0$. The cut-off energy ε_D is 1. The coupling strength is chosen from 0.0001 to 0.001. The y-intercept is given by -1.6908×10^{-8} which again indicates a good match between $\rho^{(2)}_{AC}$ and $\rho^{(2)}_{NEGF}$ in NESS.

4.2 Spinless Double Quantum Dots

Single quantum dot is a relatively simple one-levelled system. We would like to perform the analytic continuation technique to a more complicated system. Hence, as a natural generalization of single quantum dot model, the double quantum dot model can be used.

Hamiltonian

We consider two types of DQD models. For the first type, we consider each quantum dot coupled with one bath only with hopping between the two dots. For the second type, we consider one dot coupled with both the left bath and right bath with additional hopping between the two dots. For both cases, we do not consider the coulomb interaction between the two dots which can be denoted as $Ud_1^\dagger d_1 d_2^\dagger d_2$. The reason is that NEGF can only handle bilinear Hamiltonian

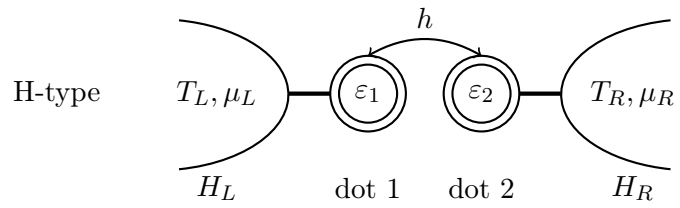

Figure 4.4: A schematic figure of an H-type double quantum dot system. Two dots with on-site energies ε_1 and ε_2 coupled to different fermionic baths in respective equilibrium with fixed temperature T_σ and chemical potential μ_σ. Electrons are allowed to hop between the two dots.

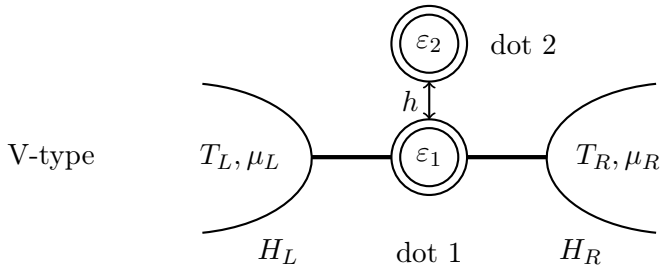

Figure 4.5: A schematic figure of an V-type double quantum dot system. The quantum dot with on-site energy ε_1 is coupled with two fermionic baths in respective equilibrium with fixed temperature T_σ and chemical potential μ_σ. Electrons are allowed to hop between the two dots.

exactly and would not be able to compare the exactness for such systems. The first type can be named as horizontal chain type (H-type) and the second type can be named as vertical chain type (V-type). They are represented by Fig. 4.4 and 4.5 below.

The Hamiltonian of H-type DQD can be cast into the following form:

$$\begin{aligned} H_{tot} &= \varepsilon_1 d_1^\dagger d_1 + \varepsilon_2 d_2^\dagger d_2 - h\left(d_1^\dagger d_2 + d_2^\dagger d_1\right) \\ &\quad + \sum_{kL} \varepsilon_{kL} c_{kL}^\dagger c_{kL} + \sum_{kR} \varepsilon_{kR} c_{kR}^\dagger c_{kR} \\ &\quad + \sum_{kL} v_{kL} d_1 c_{kL}^\dagger + \text{h.c.} \\ &\quad + \sum_{kR} v_{kR} d_2 c_{kR}^\dagger + \text{h.c.}. \end{aligned} \tag{4.24}$$

The Hamiltonian of V-type DQD can be casted in the following form:

$$\begin{aligned} H_{tot} &= \varepsilon_1 d_1^\dagger d_1 + \varepsilon_2 d_2^\dagger d_2 - h\left(d_1^\dagger d_2 + d_2^\dagger d_1\right) \\ &\quad + \sum_{kL} \varepsilon_{kL} c_{kL}^\dagger c_{kL} + \sum_{kR} \varepsilon_{kR} c_{kR}^\dagger c_{kR} \\ &\quad + \sum_{kL} v_{kL} d_1 c_{kL}^\dagger + \text{h.c.} \\ &\quad + \sum_{kR} v_{kR} d_1 c_{kR}^\dagger + \text{h.c.}. \end{aligned} \tag{4.25}$$

The only difference lies in the coupling term. The reason we propose the V-type is that it seems to mimic a SQD behavior.

Master Equation of Double Quantum Dot

The RME for H-type DQD can be referred to Appendix D.

To construct the system operator in Fock basis for arbitrary size of system, instead of identifying all the possible states transitions, we use a convenient way

$$d_i = \sigma_z^{\otimes i} \otimes d \otimes \mathbb{1}^{\otimes Z-i}, \tag{4.26}$$

where d is the annihilation operator for a single electron and d_i is the annihilation operator for the ith electron. Z represents the number of electrons the system possesses.

We would obtain four system operators namely d_1, $d_1^\dagger$, d_2, $d_2^\dagger$. In the energy eigenbasis, we denote them as S^1, S^2, S^3, S^4 respectively.

For a V-type DQD, we simply replace the system operator S^4 and the system operator S^3 which belongs to dot 2 to S^2 and S^1. The transition rate would be invariant since the baths are not changed for SQD, V-type DQD, and H-type DQD.

Nonequilibrium Green's Function for Double Quantum Dot

The retarded Green's functions for H-type and V-type DQD have the respective form

$$G_H^+ = \begin{bmatrix} \varepsilon - \varepsilon_1 - \Sigma_L^+(\varepsilon) & t \\ t & \varepsilon - \varepsilon_2 - \Sigma_R^+(\varepsilon) \end{bmatrix}^{-1}, \tag{4.27}$$

$$G_V^+ = \begin{bmatrix} \varepsilon - \varepsilon_1 - \Sigma_L^+(\varepsilon) - \Sigma_R^+(\varepsilon) & t \\ t & \varepsilon - \varepsilon_2 \end{bmatrix}^{-1}. \tag{4.28}$$

The RDM would be given as

$$\rho = \frac{\exp\left(-A_{11}d_1^\dagger d_1 - A_{12}d_1^\dagger d_2 - A_{21}d_2^\dagger d_1 - A_{22}d_2^\dagger d_2\right)}{\left[1+\exp\left(-a_1\right)\right]\left[1+\exp\left(-a_2\right)\right]}, \tag{4.29}$$

with A matrix given by $A = U^* \begin{pmatrix} a_1 & 0 \\ 0 & a_2 \end{pmatrix} U^T$ and $a_i = \ln\left(\lambda_i^{-1} - 1\right)$. λ_i is the eigenvalue of the correlation matrix D calculated.

4.2.1 Weak Coupling Limit Discussion

For DQD, it would be tedious to check if $\rho(0)$ matches analytically due to the following reasons. The solution provided by NEGF would be supplied along with basis transformations as DQD Hamiltonian no longer preserves the equivalence between Fock basis and energy eigenbasis. In addition, the solution solved via QME is already in the energy eigenbasis. A four by four matrix is required to be solved analytically and the final form would not be clear for comparison.

Instead, a numerical comparison can be done. We can directly compare the density matrix with changing parameters such as the hopping coefficient and the

chemical potential.

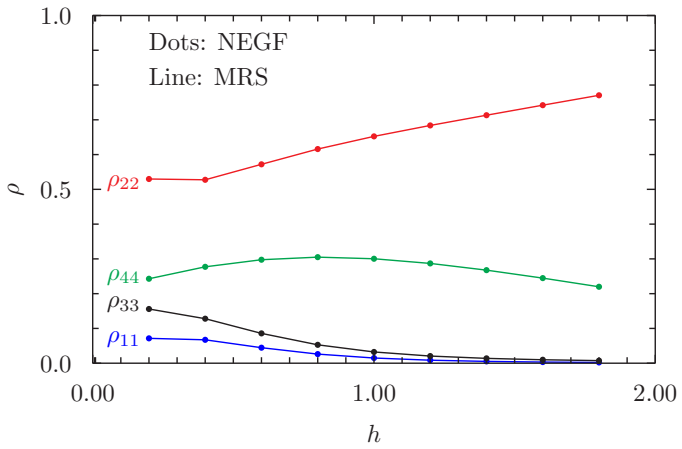

Figure 4.6: Graph of RDM as a function of hopping energy h in the weak coupling limit $\lambda^2 \to 0$; The chemical potential difference $\Delta\mu = 2$. The temperatures are set as $T_L = 0.85$ and $T_R = 0.25$. The cut-off energy $\varepsilon_D = 1$. The dot represents RDM obtained by NEGF and the line represent the RDM obtained by MRS.

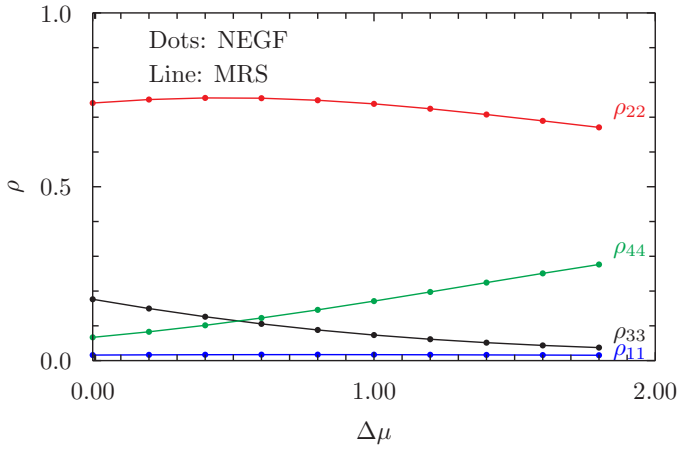

Figure 4.7: Graph of RDM as a function of chemical potential difference between the two baths $\Delta\mu$ in the weak coupling limit $\lambda^2 \to 0$; $\Delta\mu$ is defined as $\mu_L - \mu_R$. The temperatures are set as $T_L = 0.85$ and $T_R = 0.25$. Hopping coefficient $h = 1$ and the cut-off energy $\varepsilon_D = 1$. The dot represents RDM obtained by NEGF and the line represent the RDM obtained by MRS.

It can be observed that the dots that represent the NEGF result matches with the lines that Srepresent the MRS in the weak coupling limit $\lambda^2 \to 0$. Moreover, the absolute differences between the NEGF RDM and the MRS RDM are at the order 10^{-8}. A more rigorous check can be done by using the comparison scheme proposed in chapter 3 using D.E.$^{(0)}$ by varying the coupling strength.

4.2.2 Exactness Check in Equilibrium

The dimension of the Fock space of DQD will be 4 and the corresponding dimension of Hilbert space would also be 4. Hence the RDM would have 4 diagonal elements. Second order RDM would also contribute to two off-diagonal elements as conjugate pairs. The D.E.$^{(2)}$ is then checked again the 4 diagonal elements for the RDM and the real part and imaginary part of the off-diagonal elements. In equilibrium, there off-diagonal elements are zero. The discrepancy error plot is given by Fig. 4.8.

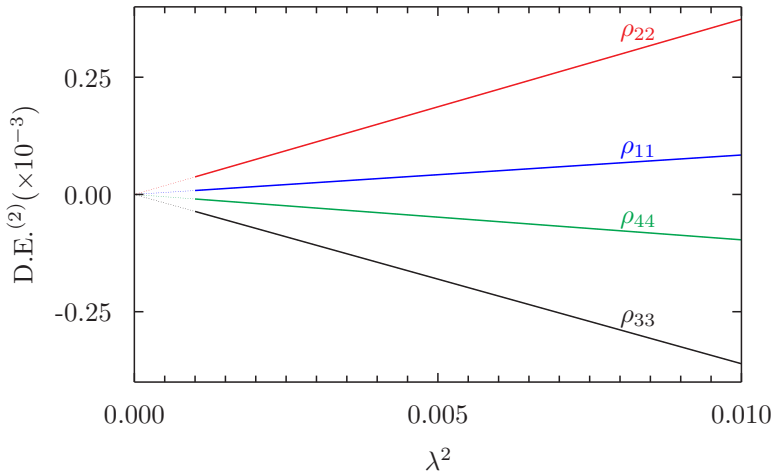

(a) H-type double quantum dot system

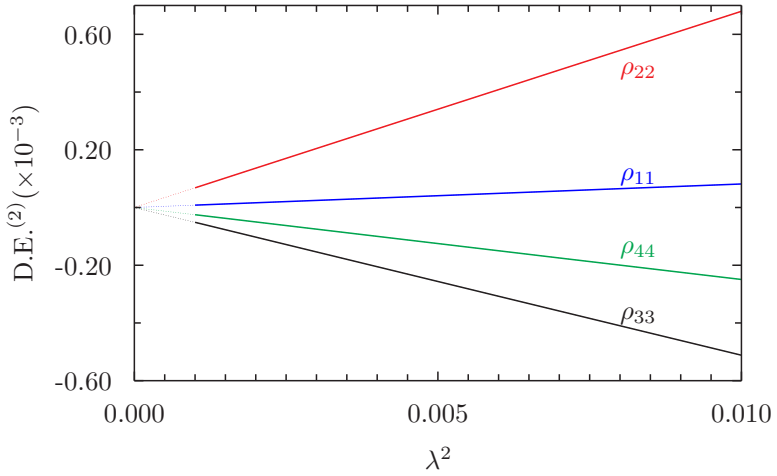

(b) V-type double quantum dot system

Figure 4.8: Figure of discrepancy error for RDM in energy eigenbasis versus system-bath coupling strength λ^2 for double quantum dot models in equilibrium; (a) represents the plot for the H-type double quantum dot. (b) represents the V-type double quantum dot. The dotted line is given by linear fitting. $T_L = 0.25$, $T_R = 0.25$ and $\mu_L = 0$, $\mu_R = 0$. The cut-off energy ε_D and the hopping energy h are chosen to be 1. The coupling strength is chosen from 0.001 to 0.01. The y-intercept for all the elements are of order 10^{-7} to 10^{-8} for both types of double quantum dot systems.

The y-intercept at the order of 10^{-7} and 10^{-8} indicates that the MRS are exact in equilibrium.

4.2.3 Exactness Check in Nonequilibrium Steady-state

A similar check is done in NESS. The plot is given by Fig. 4.9.

It can be observed that the y-intercepts for diagonal elements with second order RDM obtained via AC are at the order of 10^{-2} and 10^{-3} which ARE much larger than that in the equilibrium case. This indicates that the exactness no longer exist. For the off-diagonal elements where no manipulation is done, the y-intercepts is at the order of 10^{-8}.

We would like to investigate why there is such a loss of exactness and how would it be possible to correct the AC.

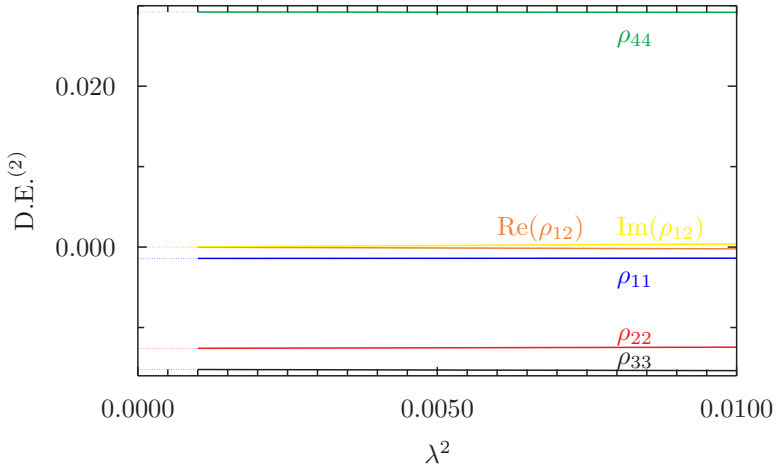

(a) H-type double quantum dot system

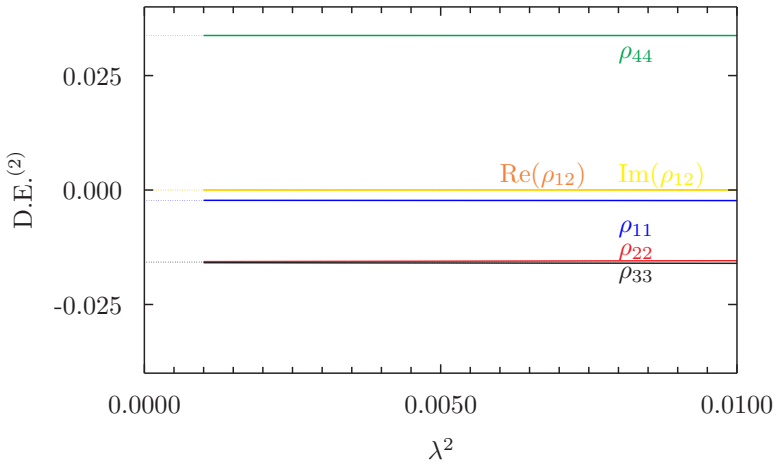

(b) H-type double quantum dot system

Figure 4.9: Figure of discrepancy error for RDM in energy eigenbasis versus system-bath coupling strength λ^2 for double quantum dot models in nonequilibrium; (a) represents the plot for the H-type double quantum dot. (b) represents the V-type double quantum dot. The dotted line is given by linear fitting. $T_L = 0.85$, $T_R = 0.25$ and $\mu_L = 2$, $\mu_R = 0$. The cut-off energy ε_D and the hopping energy h are set to 1. The coupling strength is chosen from 0.001 to 0.01. For both the H-type and V-type DQD, the y-intercept for all the diagonal elements are of order 10^{-2} to 10^{-3}. For off-diagonal elements, the y-intercept is at the order of 10^{-7}.

4.3 Correction Scheme and Failure

The MRS for DQD is not exact for second order RDM in NESS as we have illustrated. Initially, the exactness check is done for H-type DQD only. We then propose a V-type DQD which mimics a SQD except for its system size. It has been suspected that the loss of exactness is due to a sharp temperature and/or chemical potential gradient exist between the two dots for one definite system. However, the MRS solution is not exact to second order RDM again for the V-type DQD. Hence, the underlying problem may due to other possible flaws in the performing AC.

In chapter 3, the AC is performed with an expansion given by Eq. (3.24) . A seemingly harmless assumption is given by

$$\frac{\partial \rho_{nn}^{(0)}}{\partial E_i} = 0 \text{ for } i \neq n. \tag{4.30}$$

If we do not apply the above assumption, the expansion given by Eq. (3.24) should be written in the new form

$$\rho_{nn}^{(0)}(z) = \rho_{nn}^{(0)} + z\frac{\partial \rho_{nn}^{(0)}}{\partial E_n} + z\sum_{i\neq n}\frac{\partial \rho_{nn}^{(0)}}{\partial E_i}. \tag{4.31}$$

Hence our attempt is to add in the new correction term given by $z\sum_{i\neq n}\partial\rho_{nn}^{(0)}\Big/\partial E_i$. The term $\partial\rho_{nn}^{(0)}\Big/\partial E_i$ is calculated via taking partial derivative to Eq. (3.19). Without any constraints on the RDM, the attempt to solve $\partial\rho_{nn}^{(0)}\Big/\partial E_i$ would give us an underdetermined linear system. However, if the normalization condition is applied, it can be found that

$$\sum_{i}^{N}\frac{\partial \rho_{nn}^{(0)}}{\partial E_i} = 0, \tag{4.32}$$

with N as the number of energy levels.

If above statement is true, the expansion in Eq. (4.31) would be

$$\begin{aligned} \rho_{nn}^{(0)}(z) &= \rho_{nn}^{(0)} + z\sum_{i}^{N}\frac{\partial\rho_{nn}^{(0)}}{\partial E_i} \\ &= \rho_{nn}^{(0)}, \end{aligned} \tag{4.33}$$

which is not reasonable. We hence claim that Eq. (4.30) is a valid assumption.

Another attempt to correct the AC technique is by directly taking the limit for $\rho_{nm}^{(2)}$ when $\Delta_{nm} \to 0$ using L'Hospital's rule. We then find that the unnormalizaed result is given by

$$\rho_{nn}^{(2)} = \sum_{\sigma,i,\alpha\beta} 2S_{ni}^{\alpha}S_{in}^{\beta}\left[\left(-V_{in}^{''\alpha\beta}\rho_{nn}^{(0)} + V_{ni}^{''\alpha\beta}\rho_{ii}^{(0)}\right) + W_{in}^{''\alpha\beta}\frac{\partial\rho_{nn}^{(0)}}{\partial E_n}\right], \tag{4.34}$$

that is exactly twice as compared to the AC result given by Eq. (3.32). It can thus be concluded that second order RDM in MRS obtained via AC is not a mathematically well-defined limit as the limit depends on the paths chosen to approach $E_n = E_m$. The AC performed by J. Thingna in [22] fix the nth energy level and only allow the mth energy level to vary whereas L'Hospital's rule is valid when the limit is well-defined. However, it is noticed that the result obtained via L'Hospital's rule in Eq. (4.34) is identical with the Dyson expansion result supplied in [21]. It would be interesting to investigate the relation between these two results. However, these correction scheme fail to provide corrections to the MRS.

Nevertheless, the loss of exactness of MRS does not imply that it is a totally wrong answer. We would like to see in next chapter how well does MRS work as an approximation with respect to the exact solution. It would also be thought-provoking to see how does MRS perform as compared to other master equations including RME and LME.

Chapter 5

Comparison with Other Master Equations

The previous chapter gives us an indication that the exactness of modified Redfield solution does not preserve in some situations such as the double quantum dot models in nonequilibrium. However, it does not mean that this solution fails to yield a good approximation to the second order RDM. It would be interesting to compare the MRS, RME, LME and NEGF as a benchmark by using some specific physical observables. We check a few observables such as the local population of the dots and the local particle current. In this chapter, the focus will be on the H-type DQD with Hamiltonian given by Eq. (4.24).

The local population of the ith dot is simply given by

$$n_i = \left\langle d_i^\dagger d_i \right\rangle . \tag{5.1}$$

The local particle current is defined by

$$\begin{aligned} I_L &= \left\langle \frac{dN_1}{dt} \right\rangle \\ &= i \left\langle \left[d_1^\dagger d_1, H_S \right] \right\rangle \\ &= i \left\langle \left[d_1^\dagger d_1, -t \left(d_1^\dagger d_2 + d_2^\dagger d_1 \right) \right] \right\rangle \\ &= it \left\langle d_2^\dagger d_1 - d_1^\dagger d_2 \right\rangle . \end{aligned} \tag{5.2}$$

For a H-type DQD, we would like to see how various approaches would behave with respect to a varying coupling strength. The dependence of the local particle

current is plot against the coupling strength as shown in Fig. 5.1.

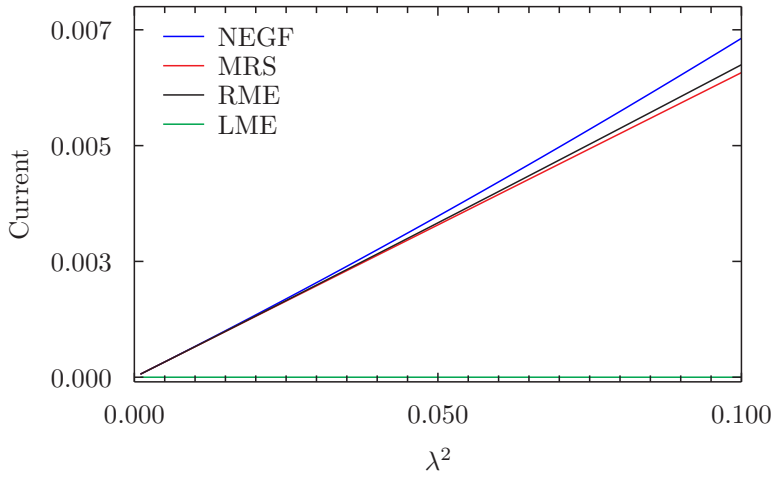

Figure 5.1: Graph of local particle current in H-type double quantum dot versus coupling strength λ^2 via Redfield master equation (Black), modified Redfield solution (Red), nonequilibrium Green's function (Blue) and Lindblad master equation (Green). The parameter used: $T_L = 0.85$, $T_R = 0.25$, $\mu_L = 2$ $\mu_R = 0$, $\varepsilon_1 = 0.2$, $\varepsilon_1 = 0.4$, $\varepsilon_D = 1$, $h = 1$.

When the coupling strength is small, the NEGF, RME and MRS approach to the same result given by $\rho^{(0)}$. When the coupling strength increases, it can be seen from the figure that the RME solution provides us a better solution as compared to MRS and LME. LME does not depend on the coupling strength and is not able to compute the local particle current for this setup. The reason is that the calculation of the defined local currents requires the off-diagonal RDM which describes the hopping process in this context. However, by performing secular approximation, the off-diagonal terms are found to be zero in steady state. This can be directly observed from Eq. (2.34). The loss of off-diagonal information would be in correspondence to the loss of information for the local current. The reason that the RME has a better solution is also due to the off-diagonal contributions from other higher order terms. By the accuracy analysis in chapter 2, we know that the second order off-diagonal elements can be determined accurately for RME. This is also evidence by the zero y-intercepts observed in

the previous chapter for the discrepancy error plots. We know that

$$\rho_{MRS} = \rho^{(0)}_{MRS} + \lambda^2 \rho^{(2)}_{MRS}, \tag{5.3}$$

$$\rho_{RME} = \rho^{(0)}_{RME} + \lambda^2 \rho^{(2)}_{RME} + \lambda^4 \rho^{(4)}_{RME} + \cdots, \tag{5.4}$$

where $\rho^{(0)}$ does not contain off-diagonal elements as we have shown in chapter 3. The contribution of the off-diagonal elements would come from $\rho^{(2)}$ that are exact for both the MRS and RME. However, RME also contains the off-diagonal elements from higher order terms even though they are incorrectly determined. Hence, as compared to the MRS with $\rho^{(2)}_{od}$ only, the RME with $\rho^{(2)}_{od} + \rho^{(\text{higher orders})}_{od}$ is expected to have a better result as compared to MRS. The points out a limitation for MRS when the calculation of certain observables requires the off-diagonal contribution.

From the plots of the population as shown in Fig. 5.2, again the NEGF, RME, MRS and LME approach to the same value when the coupling strength is small as a consequence of the equivalence in weak coupling limit. With a higher coupling strength, the MRS results are consistently smaller than that of NEGF. Meanwhile, the RME results are consistently larger. In contrast, LME only gives a correct description of the population distribution in the weak coupling limit.

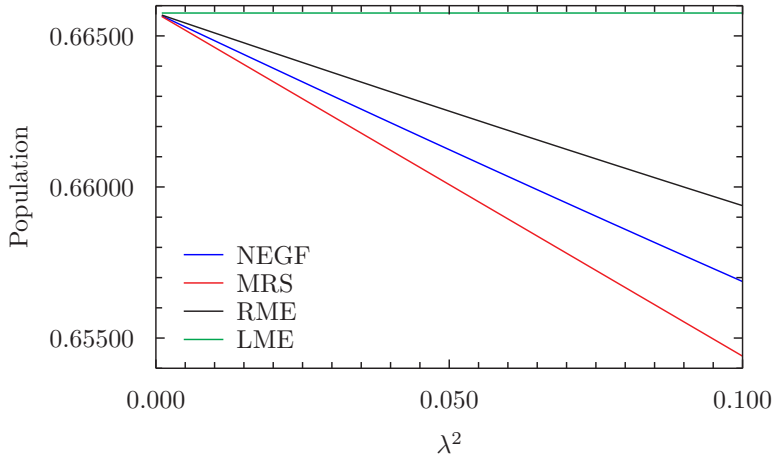

(a) Population of dot 1

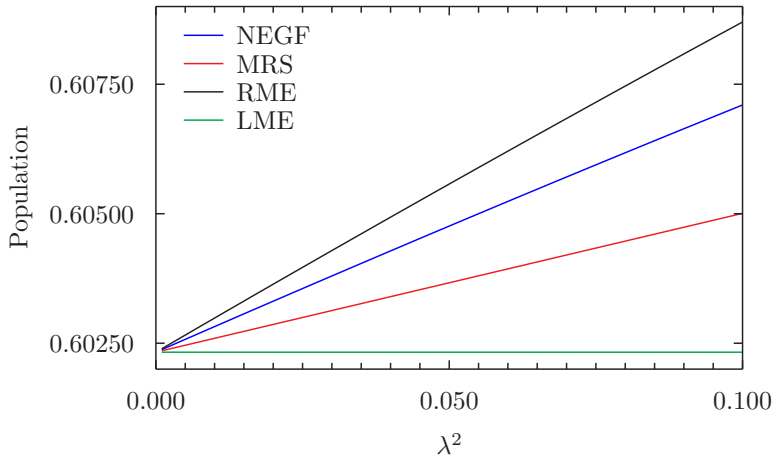

(b) Population of dot 2

Figure 5.2: Graph of population of dot 1 and dot 2 in H-type double quantum dot versus coupling strength λ^2 via Redfield master equation (Black), modified Redfield solution (Red), nonequilibrium Green's function (Blue) and Lindblad master equation (Green). The parameter used: $T_L = 0.85$, $T_R = 0.25$, $\mu_L = 2$, $\mu_R = 0$, $\varepsilon_1 = 0.2$, $\varepsilon_2 = 0.4$, $\varepsilon_D = 1$, $h = 1$.

The dependence of the local current on the coupling strength is revealed. However, in our problem, we always consider the left bath and the right bath to be symmetric with identical spectral density and coupling strength. Variation of the coupling strength occurs symmetrically.

We consider another situation by varying the chemical potential which is equivalent to variation of the degree of bias of the system.

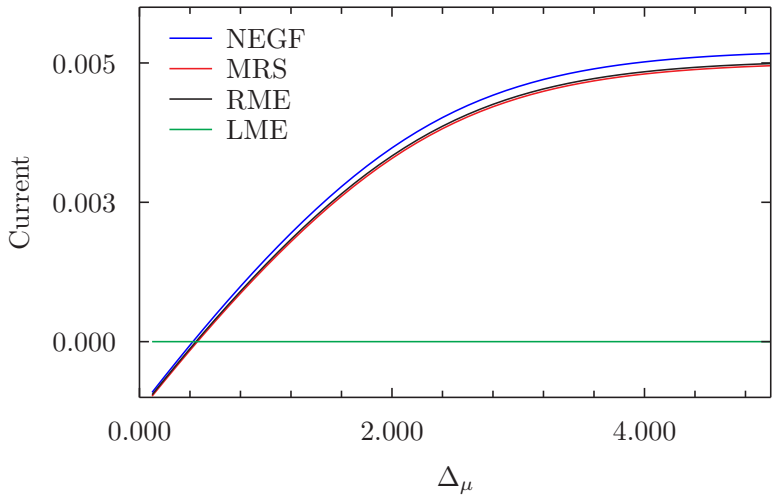

Figure 5.3: Graph of local particle current in H-type double quantum dot versus chemical potential difference $\Delta\mu$ via Redfield master equation (Black), modified Redfield solution (Red), nonequilibrium Green's function (Blue) and Lindblad master equation (Green). The parameter used: $T_L = 0.85$, $T_R = 0.25$, λ^2=0.05, $\varepsilon_1 = 0.2$, $\varepsilon_2 = 0.4$, $\varepsilon_D = 1$, $h = 1$.

The local particle current is plotted against the chemical potential difference in Fig. 5.3 the RME have a result that is closer the that of NEGF. The local population profile given by Fig. 5.4 gives a similar conclusion in the previous case that the MRS is always smaller the solution of NEGF and RME is always larger. When the chemical potential increases, the system would be in a stronger nonequilibrium condition and the difference between various solution will be greater.

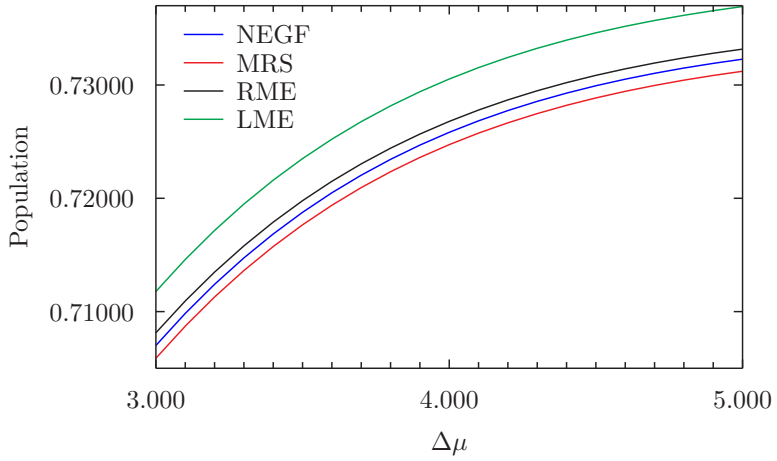

(a) Population of dot 1

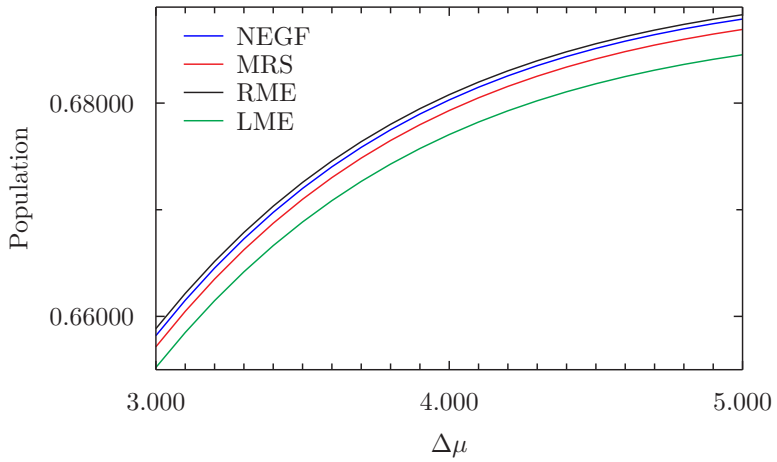

(b) Population of dot 2

Figure 5.4: Graph of local population of dot 1 and dot 2 in H-type double quantum dot versus chemical potential difference $\Delta\mu$ via Redfield master equation (Black), modified Redfield solution (Red), nonequilibrium Green's function (Blue) and Lindblad master equation (Green). The parameter used: $T_L = 0.85$, $T_R = 0.25$, λ^2=0.05, $\varepsilon_1 = 0.2$, $\varepsilon_2 = 0.4$, $\varepsilon_D = 1$, $h = 1$.

The above chosen observables do not give a clear indication of the accuracy of MRS as compared to RME. The RME discrepancy error plot is compared with the MRS discrepancy error plot in Fig. 5.5.

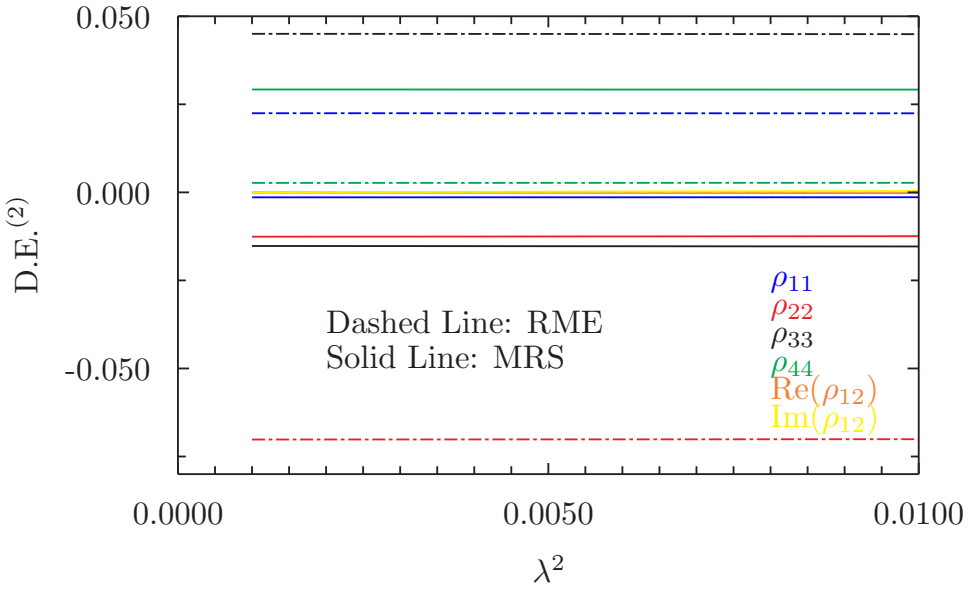

Figure 5.5: Figue of discrepancy error for RDM in energy eigenbasis versus the system-bath coupling strength an H-type double quantum dot; The solid line represents the result for MRS. The dashed line represents the result for RME. $T_L = 0.85$, $T_R = 0.25$ and $\mu_L = 2$, $\mu_R = 0$. The cut-off energy ε_D is 1. The coupling strength is chosen from 0.001 to 0.1.

We can see from the plot that the RME results have a larger y-intercept as compared to RME for the diagonal elements of the second order RDM except for ρ_{44}. It means that it deviates from the exact value more than MRS. Hence, MRS is more accurate than RDM for second order RDM in weak coupling regime. Since the local population plot is not able to give us a clear indication on whether RME or MRS is a better solution due to their consistent deviation, we check the global population for all the energy levels. The global population plot is given by Fig. 5.6. It can be seen that the global population gives a good match for MRS and NEGF for the first three energy levels. However, the population for the fourth energy level has a great deviation for MRS. This is also indicated by the discrepancy error plot. As compared to RME, MRS still give a better predication for most of the energy levels. The breakdown of MRS for a certain level may be a clue to investigate the flaw in AC.

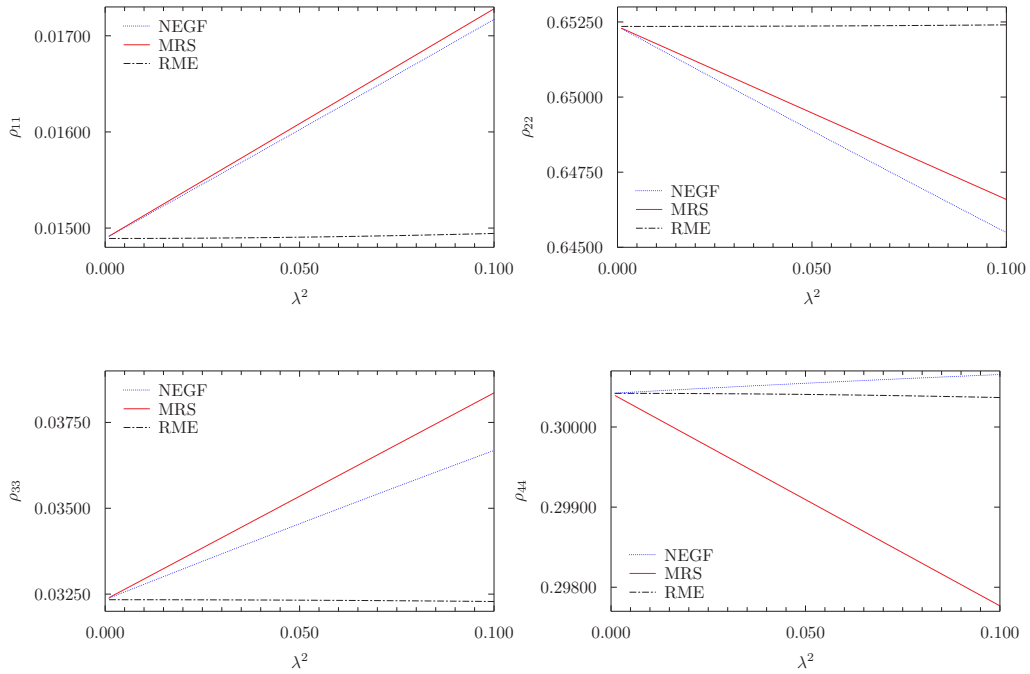

Figure 5.6: Graph of populations for all the energy levels versus the coupling strength; The red line represents the result for MRS. The black dashed line represents the result for RME. The blue dotted line represent the result for NEGF. $T_L = 0.85$, $T_R = 0.25$ and $\mu_L = 2$, $\mu_R = 0$. The cut-off energy ε_D is 1. The coupling strength is chosen from 0.001 to 0.1.

Moreover, it is noticed that RME would break down when the coupling strength is strong if we consider the occupation number in different energy eigenstate. An example is given by Fig. 5.7. It can be seen that the RME solution no longer preserves positivity whereas the positivity for MRS still holds. For local observable like population for dot 1 and dot 2. Such loss of positivity for RME is not easy to observed if local population is considered as it would be cancelled by contribution from other elements of RDM. A more detailed study on the valid regime of RME can be done together with MRS.

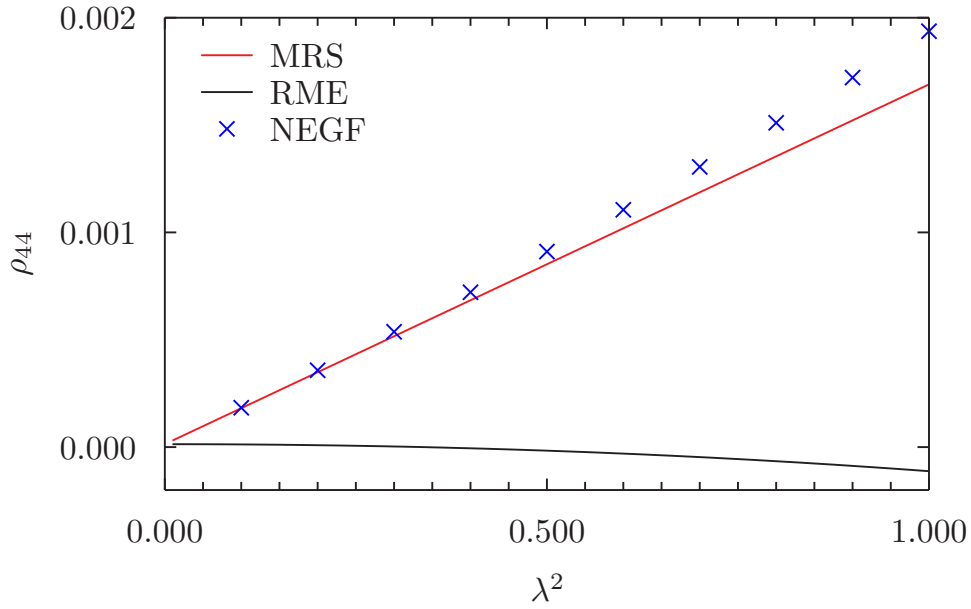

Figure 5.7: Graph of RDM versus coupling strength λ^2; $T_L = 0.45$ $T_R = 0.25$ and $\mu_L = 1$ $\mu_R = 0$.The on-site energies are $\varepsilon_1 = 2$ and $\varepsilon_2 = 4$. The coupling strength is chosen from 0.01 to 1. The blue cross represents the NEGF solution. The red line represents the MRS and the black line represents the RME solution.

Chapter 6

Conclusion

In conclusion, we have extended the modified Redfield solution to fermionc systems by performing analytic continuation technique. More specifically, the exactness of the MRS in nonequilibrium steady-state has been examined. The MRS in general does not preserve exactness. For a single quantum dot, the MRS provides us with exact solution up to second order RDM in both equilibrium and NESS. An exact match for the zeroth order RDM can be shown analytically as compared to NEGF in the weak coupling limit. The SQD model does not reveal a complicated physical scenario as it is only one-levelled systen with a fixed energy spacing. It follows that multi-levelled double quantum dot models with two different configurations are studied. A numerical study is done in the weak coupling limit which verifies that the zeroth order RDM is exact. For both types of DQD models, the exactness of second order RDM still preserves in equilibrium. In NESS, the exactness no longer preserves as evident by discrepancy error which is 10^5 order greater than exact case. A possible correction scheme on the expansion of zeroth order RDM has shown to be failed. However, such scheme provides a good support on the assumption made in previous work of MRS. Another attempt to make an alternative formalism of analytic continuation technique provides an answer with a factor of two difference which corresponds to results obtained via Dyson expansion.

Though the modified Redfield solution is unable to produced an exact solution in general, it would be interesting to see how well does MRS improve on the results obtained from RME and LME. By demonstrating on an H-type DQD,

the result on local current shows that the MRS tend to have larger deviations from the exact result as compared to RME. These results provide us with an important piece of information that the higher order contribution of RDM is more important than the accuracy contribution to limited orders. Studies on the local population of the dots do not provide a clear-cut evidence on the performance of MRS and RME. The results for global population indicate that the MRS is better as compared to RME in most situation. Moreover, the positivity of RDM of RME would break down at large coupling strength as compared to MRS and NEGF. The validity of RDM and MRS could be studies more thoroughly by considering different observables.

In general, the modified Redfield solution provide as possible solution to obtain the second order RDM without going into higher order calculation. It would be interesting to continue to investigate the exactness of this approach. One possible future work could be done is to provide an analytical proof for the exactness of MRS in equilibrium for fermionic systems as inspired by the case for systems with bosonic baths. It is also possible to continue to work on zeroth order RDM correction scheme as the expansion of such zeroth order RDM is subtle. Other possible systems could be proposed such as a triple quantum dot model which help us to analyse possible flaw in the approach by increasing complexity of the system. With the results in last chapter, it would be interesting for us to investigate a possible solution which contains higher order contribution as well as a second order result that is supplied by MRS. Such solution would intuitively provide a correction on RME.

References

[1] Karl Blum. *Density matrix theory and applications*, volume 64. Springer Science & Business Media, 2012.

[2] Heinz-Peter Breuer and Francesco Petruccione. *The theory of open quantum systems*. Oxford University Press on Demand, 2002.

[3] Hans-Jürgen Briegel and Berthold-Georg Englert. Quantum optical master equations: The use of damping bases. *Physical Review A*, 47(4):3311, 1993.

[4] Howard Carmichael. *An open systems approach to quantum optics: lectures presented at the Université Libre de Bruxelles, October 28 to November 4, 1991*, volume 18. Springer Science & Business Media, 2009.

[5] Abhishek Dhar, Keiji Saito, and Peter Hänggi. Nonequilibrium density-matrix description of steady-state quantum transport. *Physical Review E*, 85(1):011126, 2012.

[6] Chris H Fleming and Nick I Cummings. Accuracy of perturbative master equations. *Physical Review E*, 83(3):031117, 2011.

[7] Vittorio Gorini, Andrzej Kossakowski, and Ennackal Chandy George Sudarshan. Completely positive dynamical semigroups of n-level systems. *Journal of Mathematical Physics*, 17(5):821–825, 1976.

[8] Upendra Harbola, Massimiliano Esposito, and Shaul Mukamel. Quantum master equation for electron transport through quantum dots and single molecules. *Physical Review B*, 74(23):235309, 2006.

[9] Hartmut Haug, Antti-Pekka Jauho, and M Cardona. *Quantum kinetics in transport and optics of semiconductors*, volume 14. Springer, 2008.

[10] Roman S Ingarden, Andrzej Kossakowski, and Masanori Ohya. *Information dynamics and open systems: classical and quantum approach*, volume 86. Springer Science & Business Media, 2013.

[11] Seogjoo Jang, Jianshu Cao, and Robert J Silbey. Fourth-order quantum master equation and its markovian bath limit. *The Journal of chemical physics*, 116(7):2705–2717, 2002.

[12] Leo P Kouwenhoven, DG Austing, and Seigo Tarucha. Few-electron quantum dots. *Reports on Progress in Physics*, 64(6):701, 2001.

[13] Ryogo Kubo, Morikazu Toda, and Natsuki Hashitsume. *Statistical physics II: nonequilibrium statistical mechanics*, volume 31. Springer Science & Business Media, 2012.

[14] Lev Landau. Das dämpfungsproblem in der wellenmechanik. *Zeitschrift für Physik*, 45(5-6):430–441, 1927.

[15] Goran Lindblad. On the generators of quantum dynamical semigroups. *Communications in Mathematical Physics*, 48(2):119–130, 1976.

[16] Takashi Mori and Seiji Miyashita. Dynamics of the density matrix in contact with a thermal bath and the quantum master equation. *Journal of the Physical Society of Japan*, 77(12):124005, 2008.

[17] Sadao Nakajima. On quantum theory of transport phenomena steady diffusion. *Progress of Theoretical Physics*, 20(6):948–959, 1958.

[18] Wolfgang Pauli. Festschrift zum 60. geburtstage a. sommerfelds. *Hirzel, Leipzig*, 30, 1928.

[19] Alfred G. Redfield. On the theory of relaxation processes. *IBM Journal of Research and Development*, 1(1):19–31, 1957.

[20] Gernot Schaller. *Open Quantum Systems Far from Equilibrium*, volume 881. Springer, 2014.

[21] Juzar Thingna. *Steady-state transport properties of anharmonic systems*. PhD thesis, Ph. D. thesis, National University Singapore, 2013.

[22] Juzar Thingna, Jian-Sheng Wang, and Peter Hänggi. Generalized gibbs state with modified redfield solution: Exact agreement up to second order. *The Journal of chemical physics*, 136(19):194110, 2012.

[23] Juzar Thingna, Jian-Sheng Wang, and Peter Hänggi. Reduced density matrix for nonequilibrium steady states: A modified redfield solution approach. *Physical Review E*, 88(5):052127, 2013.

[24] Juzar Thingna, Hangbo Zhou, and Jian-Sheng Wang. Improved dyson series expansion for steady-state quantum transport beyond the weak coupling limit: Divergences and resolution. *The Journal of chemical physics*, 141(19):194101, 2014.

[25] Wilfred G van der Wiel, Silvano De Franceschi, Jeroen M Elzerman, Toshimasa Fujisawa, Seigo Tarucha, and Leo P Kouwenhoven. Electron transport through double quantum dots. *Reviews of Modern Physics*, 75(1):1, 2002.

[26] John Von Neumann. Wahrscheinlichkeitstheoretischer aufbau der quantenmechanik. *Nachrichten von der Gesellschaft der Wissenschaften zu Göttingen, Mathematisch-Physikalische Klasse*, 1927:245–272, 1927.

[27] Jian-Sheng. Wang, Bijay Kumar. K. Agarwalla, Huanan Li, and Juzar Thingna. Nonequilibrium greens function method for quantum thermal transport. *Frontiers of Physics*, 9(6):673–697, 2014.

[28] Ulrich Weiss. *Quantum dissipative systems*, volume 10. World Scientific, 1999.

[29] David Zueco. Quantum and statistical mechanics in open systems: theory and examples. *arXiv preprint arXiv:0908.3698*, 2009.

[30] Robert Zwanzig. Ensemble method in the theory of irreversibility. *The Journal of Chemical Physics*, 33(5):1338–1341, 1960.

Appendix A

Proof of Kubo Identity

The Kubo identity has the following expression:

$$e^{\beta\left(\hat{A}+\hat{B}\right)} = e^{\beta\hat{A}}\left[\mathbb{1}+\int_0^\beta d\tau e^{-\tau\hat{A}}\hat{B}e^{\tau\left(\hat{A}+\hat{B}\right)}\right] \tag{A.1}$$

Consider $e^{-\beta\hat{A}}\hat{B}e^{\beta\left(\hat{A}+\hat{B}\right)}$,

$$\begin{aligned} e^{-\beta\hat{A}}\hat{B}e^{\beta\left(\hat{A}+\hat{B}\right)} &= -\hat{A}e^{-\beta\hat{A}}e^{\beta\left(\hat{A}+\hat{B}\right)}+e^{-\beta\hat{A}}\left(\hat{A}+\hat{B}\right)e^{\beta\left(\hat{A}+\hat{B}\right)} \\ &= \frac{d}{d\beta}\left[e^{-\beta\hat{A}}e^{\beta\left(\hat{A}+\hat{B}\right)}\right] \end{aligned} \tag{A.2}$$

$$\int_0^\beta d\tau e^{-\tau\hat{A}}\hat{B}e^{\tau\left(\hat{A}+\hat{B}\right)} = e^{-\beta\hat{A}}e^{\beta\left(\hat{A}+\hat{B}\right)} \tag{A.3}$$

$$\mathbb{1}+\int_0^\beta d\tau e^{-\tau\hat{A}}\hat{B}e^{\tau\left(\hat{A}+\hat{B}\right)} = e^{-\beta\hat{A}}e^{\beta\left(\hat{A}+\hat{B}\right)} \tag{A.4}$$

$$e^{\beta\hat{A}}\left[\mathbb{1}+\int_0^\beta d\tau e^{-\tau\hat{A}}\hat{B}e^{\tau\left(\hat{A}+\hat{B}\right)}\right] = e^{\beta\left(\hat{A}+\hat{B}\right)} \tag{A.5}$$

which is exactly the Kubo identity.

Appendix B

Bath Correlators and Transition Rates

The bath correlator $C^{\alpha\beta}(t)$ is defined as $\left\langle \tilde{B}^{\alpha}(t) B^{\beta}(0) \right\rangle$. For electronic baths, we have

$$B_{\sigma}^{1} = \sum_{k\sigma} v_{k\sigma} c_{k\sigma}^{\dagger}, \tag{B.1}$$

$$B_{\sigma}^{2} = \sum_{k\sigma} v_{k\sigma}^{*} c_{k\sigma}^{\dagger}. \tag{B.2}$$

It follows that

$$\begin{aligned} C_{\sigma}^{\alpha\beta}(t) &= \left\langle \tilde{B}_{\sigma}^{\alpha}(t) B_{\sigma}^{\beta}(0) \right\rangle. \\ &= \mathrm{Tr_B}\left[\rho_B \tilde{B}_{\sigma}^{\alpha}(t) B_{\sigma}^{\beta}(0) \right]. \end{aligned} \tag{B.3}$$

The non-vanishing correlations are $C_{\sigma}^{12}(t)$ and $C_{\sigma}^{21}(t)$ as the other terms are $\left\langle c_{k\sigma}^{\dagger}(t) c_{k\sigma}^{\dagger} \right\rangle$ and $\langle c_{k\sigma}(t) c_{k\sigma} \rangle$ which are zero.

$$\begin{aligned} C_{\sigma}^{12}(t) &= \mathrm{Tr_B}\left[\rho_B \tilde{B}_{\sigma}^{\alpha}(t) B_{\sigma}^{\beta}(0) \right] \\ &= \sum_{k\sigma} |v_{k\sigma}|^2 \mathrm{Tr_B}\left(\rho_B c_{k\sigma}^{\dagger} c_{k\sigma} \right) e^{i\varepsilon_k t} \\ &= \int_{-\infty}^{\infty} \frac{d\varepsilon}{2\pi} 2\pi \sum_{k\sigma} |v_{k\sigma}|^2 \delta(\varepsilon - \varepsilon_k) f_{\sigma}(\varepsilon) e^{i\varepsilon t} \\ &= \int_{-\infty}^{\infty} \frac{d\varepsilon}{2\pi} \Gamma_{\sigma}(\varepsilon) f_{\sigma}(\varepsilon) e^{i\varepsilon t}. \end{aligned} \tag{B.4}$$

Similarly, we have

$$C_{\sigma}^{21}(t) = \int_{-\infty}^{\infty} \frac{d\varepsilon}{2\pi} \Gamma_{\sigma}(\varepsilon) [1 - f_{\sigma}(\varepsilon)] e^{-i\varepsilon t}, \tag{B.5}$$

where $\Gamma_{\sigma}(\varepsilon) = 2\pi \sum_{k\sigma} |v_{k\sigma}|^2 \delta(\varepsilon - \varepsilon_k)$ is known as the spectral density and $f_{\sigma}(\varepsilon)$ is the Fermi-Dirac distribution of the bath σ at T_{σ} and μ_{σ}. Hence $f_{\sigma}(\varepsilon)$ is given by $\{\exp[(\varepsilon - \mu_{\sigma})/T_{\sigma}] + 1\}^{-1}$The spectral density is approximated as a Lorentzian with the following form

$$\Gamma_{\sigma}(\varepsilon) = \frac{\Gamma_{\sigma}}{1 + \left(\frac{\varepsilon}{\varepsilon_D}\right)^2}, \tag{B.6}$$

where ε_D is cut-off energy.

$C_{\sigma}^{12}(t)$ would then take the form

$$C_{\sigma}^{12}(t) = \int_{-\infty}^{\infty} \frac{d\varepsilon}{2\pi} \frac{\Gamma_{\sigma}}{1 + \left(\frac{\varepsilon}{\varepsilon_D}\right)^2} \frac{1}{\exp[(\varepsilon - \mu_{\sigma})/T_{\sigma}] + 1} e^{i\varepsilon t}. \tag{B.7}$$

The above integral can then be calculated using residue theorem. The poles are given by

$$\varepsilon_{+} = i\varepsilon_D, \tag{B.8}$$

$$\varepsilon_{-} = -i\varepsilon_D, \tag{B.9}$$

$$\varepsilon_{l_+} = i\nu_{\sigma l+} + \mu_{\sigma}, \tag{B.10}$$

$$\varepsilon_{l_-} = i\nu_{\sigma l-} + \mu_{\sigma}, \tag{B.11}$$

where $\nu_l = \pi(2l + 1) T_{\sigma}$ is known as the Matsubara frequency and $l_+ = 0$, 1, 2 ,3$\cdots$ and l_- are all the negative integers. The sign+ indicates that the poles are on the upper half complex plane and - for the poles in the lower complex plane. We takes the poles in the upper half plane as the integral diverges using the poles in the lower half plane due to the existence of $e^{i\varepsilon t}$ term. By evaluating

the residues, it can be found that

$$C_{\sigma}^{12}(t) = \frac{\Gamma_{\sigma}\varepsilon_D}{2} f_{\sigma}(i\varepsilon_D)\, e^{-\varepsilon_D t} - iT_{\sigma}\sum_{l_+}\Gamma_{\sigma}\left(\varepsilon_{l_+}\right) e^{i\varepsilon_{l_+}t}, \tag{B.12}$$

$$C_{\sigma}^{21}(t) = \frac{\Gamma_{\sigma}\varepsilon_D}{2} e^{-\varepsilon_D t} - C_{\sigma}^{12*}(t). \tag{B.13}$$

We also have the relation $C_{\sigma}^{12*}(t) = C_{\sigma}^{12}(-t)$ if we try to evaluate $C_{\sigma}^{12*}(t)$ using the poles in the lower half plane. The system-bath coupling λ^2 is always absorbed in the bath correlator.

By using the definition of W given by Eq. (2.25), W can be found by

$$W_{\sigma ij}^{12} = \frac{\Gamma_{\sigma}\varepsilon_D}{2} f_{\sigma}(i\varepsilon_D)\frac{1}{(i\Delta_{ij}+\varepsilon_D)} - T_{\sigma}\sum_{l_+}\Gamma_{\sigma}\left(\varepsilon_{l_+}\right)\frac{1}{\left(\Delta_{ij}-\varepsilon_{l_+}\right)}, \tag{B.14}$$

$$W_{\sigma ij}^{21} = \frac{\Gamma_{\sigma}\varepsilon_D}{2(i\Delta_{ij}+\varepsilon_D)} - W_{\sigma ji}^{12*}. \tag{B.15}$$

Hence the transition rates can be found via taking the real parts of above results.

It follows that $V_{\sigma ij}^{12}$ can be found via $\partial W_{\sigma ij}^{12}/\Delta_{ij}$ defined in chapter 2.

Appendix C

Lindblad Master Equation Equivalent Form

In chapter 2, we obtain the RME as given by Eq. (2.22). We define the dissipative term as a *dissipator* $\mathcal{D}[\rho(t)]$

$$\mathcal{D}[\rho(t)] = -\sum_{\sigma\alpha\beta}\int_0^t d\tau \left\{\left[S^\alpha, \tilde{S}^\beta(\tau - t)\,\rho(t)\right] C^{\alpha\beta}(t-\tau) + \text{h.c.}\right\}. \quad \text{(C.1)}$$

By performing secular approximation, the above equation can be cast into Lindblad form. The secular approximation is also known as rotating wave approximation (RWA) . RWA is performed on the level of Hamiltonian whereas for secular approximation, it is performed on the level of master equation.

By defining new operators

$$S(\Delta_{ij}) = \sum_{E_i - E_j = \Delta_{ij}} |E_i\rangle\langle E_i| S |E_j\rangle\langle E_j|. \quad \text{(C.2)}$$

The time evolution of the new operator takes the form

$$\langle E_j|\tilde{S}(\Delta_{ij}, t)|E_i\rangle = e^{i\Delta_{ij}t} S(\Delta_{ij}). \quad \text{(C.3)}$$

The dissipator then takes the following form

$$\begin{aligned}
& \mathcal{D}\left[\rho\left(t\right)\right] \\
= & \sum_{\sigma\alpha\beta}\int_{0}^{t}d\tau\Big\{\left[S^{\alpha},\tilde{S^{\beta}}\left(\tau-t\right)\rho\left(t\right)\right]C^{\alpha\beta}\left(t-\tau\right) \\
& -\left[S^{\beta},\rho\left(t\right)\tilde{S^{\alpha}}\left(\tau-t\right)\right]C^{\alpha\beta}\left(\tau-t\right)\Big\} \\
= & \sum_{\sigma\alpha\beta}\sum_{\Delta_{ij},\Delta_{nm}}\int_{0}^{t}d\tau\Big\{\left[S^{\alpha}\left(\Delta_{ij}\right),S^{\beta}\left(\Delta_{nm}\right)\rho\left(t\right)\right]e^{i\Delta_{nm}(\tau-t)}C^{\alpha\beta}\left(t-\tau\right) \\
& -\left[S^{\beta}\left(\Delta_{ij}\right),\rho\left(t\right)S^{\alpha}\left(\Delta_{nm}\right)\right]e^{i\Delta_{nm}(\tau-t)}C^{\alpha\beta}\left(\tau-t\right)\Big\}. \qquad \text{(C.4)}
\end{aligned}$$

By using secular approximation where we simply retain the term $\Delta_{nm}=\Delta_{ij}$ as the rest of terms in total averages to zero,

$$\begin{aligned}
& \mathcal{D}\left[\rho\left(t\right)\right] \\
= & \sum_{\sigma\alpha\beta}\sum_{\Delta_{ij}}\Big\{\left[S^{\alpha}\left(\Delta_{ij}\right),S^{\beta}\left(\Delta_{ij}\right)\rho\left(t\right)\right]\int_{0}^{t}d\tau e^{i\Delta_{ij}(\tau-t)}C^{\alpha\beta}\left(t-\tau\right) \\
& -\left[S^{\beta}\left(\Delta_{ij}\right),\rho\left(t\right)S^{\alpha}\left(\Delta_{ij}\right)\right]\int_{0}^{t}d\tau e^{i\Delta_{ij}(\tau-t)}C^{\alpha\beta}\left(\tau-t\right)\Big\} \\
= & \sum_{\sigma\alpha\beta}\sum_{\Delta_{ij}}\Big\{W_{ij}^{\alpha\beta}\left[S^{\alpha}\left(\Delta_{ij}\right),S^{\beta}\left(\Delta_{ij}\right)\rho\right] \\
& -\left[S^{\beta}\left(\Delta_{ij}\right),\rho S^{\alpha}\left(\Delta_{ij}\right)\right]W_{ij}^{\alpha\beta*}\Big\} \\
= & \sum_{\sigma\alpha\beta}\sum_{\Delta_{ij}}2W_{ij}^{'\alpha\beta}\left(S^{\beta}\left(\Delta_{ij}\right)\rho S^{\alpha}\left(\Delta_{ij}\right)-\frac{1}{2}\left\{S^{\alpha}\left(\Delta_{ij}\right)S^{\beta}\left(\Delta_{ij}\right),\rho\right\}\right) \\
& -\sum_{\sigma\alpha\beta}\sum_{\Delta_{ij}}\frac{i}{\hbar}\left[H_{LS},\rho\right], \qquad \text{(C.5)}
\end{aligned}$$

where

$$H_{LS} \;=\; \sum_{\sigma}\sum_{\alpha\beta}\sum_{\Delta_{ij}}W_{ij}^{''\alpha\beta}S^{\alpha}\left(\Delta_{ij}\right)S^{\beta}\left(\Delta_{ij}\right). \qquad \text{(C.6)}$$

H_{LS} is often call as the *lamb shift* term which give a renormalization of the energy levels. $[H_{LS},H_S]=0$ and such renormalization is often neglected.

This is exactly the Lindblad Form if we compare it with the result obtained by quantum dynamical semigroup [2, 15, 7].

$$\mathcal{L}\rho = -i\left[H,\rho\right] + \sum_{k=1}^{N^2-1} \gamma_k \left(A_k \rho A_k^\dagger - \frac{1}{2} A_k^\dagger A_k \rho - \frac{1}{2} \rho A_k^\dagger A_k \right). \qquad \text{(C.7)}$$

Appendix D

Redfield Master Equation for H-type Double Quantum Dot

The Redfield master equation of an H-type double quantum dot in its eigenenergy basis reads

$$
\begin{aligned}
& \frac{d\rho_{nm}}{dt} \\
= \; & -i\Delta_{nm}\rho_{nm}(t) \\
& + \sum_{ij} \Big[S^2_{ni} S^1_{jm} W^{21*}_{L,mj} + S^2_{ni} S^1_{jm} W^{21}_{L,ni} \\
& - \delta_{m,j} \sum_l S^2_{nl} S^1_{li} W^{12}_{L,li} - \delta_{i,n} \sum_l S^2_{jl} S^1_{lm} W^{12*}_{L,lj} \\
& + S^1_{ni} S^2_{jm} W^{12}_{L,ni} + S^1_{ni} S^2_{jm} W^{12*}_{L,mj} \\
& - \delta_{i,n} \sum_l S^1_{jl} S^2_{lm} W^{21*}_{L,lj} - \delta_{m,j} \sum_l S^1_{nl} S^2_{li} W^{43}_{L,li} \\
& + S^4_{ni} S^3_{jm} W^{43*}_{R,mj} + S^4_{ni} S^3_{jm} W^{43}_{R,ni} \\
& - \delta_{m,j} \sum_l S^4_{nl} S^3_{li} W^{34}_{R,li} - \delta_{i,n} \sum_l S^4_{jl} S^3_{lm} W^{34*}_{R,lj} \\
& + S^3_{ni} S^4_{jm} W^{34}_{R,ni} + S^3_{ni} S^4_{jm} W^{34*}_{R,mj} \\
& - \delta_{i,n} \sum_l S^3_{jl} S^4_{lm} W^{43*}_{R,lj} - \delta_{m,j} \sum_l S^3_{nl} S^4_{li} W^{43}_{R,li} \Big] \rho_{ij}
\end{aligned}
\tag{D.1}
$$

where $S^{1,2,3,4}$ are the system operators in the energy eigenbasis. S^1 and S^2 are the system operators of the dot 1. S^3 and S^4 are the system operators of the dot 2. For an V-type double quantum dot, simply replace the system operator S^3 and S^4 with S^1 and S^2 as the dot 2 is no longer coupled with any bath.

Appendix E

Self Energy of Fermionic Bath

Spectral density $\Gamma_\sigma(\varepsilon)$ is given as

$$\Gamma_\sigma(\varepsilon) = \frac{\Gamma_\sigma}{1+\left(\frac{\varepsilon}{\varepsilon_D}\right)^2}. \tag{E.1}$$

The self-energies can be calculated which gives

$$\Sigma_\sigma^+(\varepsilon) = \frac{1}{2}\frac{\varepsilon\varepsilon_D\Gamma_\sigma}{\varepsilon^2+\varepsilon_D^2} - \frac{1}{2}\frac{\varepsilon_D^2\Gamma_\sigma}{\varepsilon^2+\varepsilon_D^2}. \tag{E.2}$$

By using Dyson equation,

$$G^+(\varepsilon) = g^+(\varepsilon) + g^+(\varepsilon)\left(\sum_\sigma \Sigma_\sigma^+(\varepsilon)\right) G^+(\varepsilon) \tag{E.3}$$

The Green's function of the sinlge quantum dot can be expressed as

$$\begin{aligned} G^+(\varepsilon) &= \frac{1}{g^{-1}(\varepsilon) - \sum_\sigma \Sigma_\sigma^+(\varepsilon)} \\ &= \frac{1}{\varepsilon - \varepsilon_0 - \sum_\sigma \Sigma_\sigma^+(\varepsilon) + i\eta}. \end{aligned} \tag{E.4}$$

Appendix F

List of Codes and Sample Codes

List of codes used

1. Analytic NEGF Fortran codes to calculate exact RDM (By the author)
2. Semi-analytic NEGF Mathematica programme to calculate exact RDM (By the author)
3. Numerical NEGF Mathematica programme to calculate exact RDM (By the author)
4. RME codes in Fortran to calculate RDM for SQD and DQD (By the author)
5. LME codes in Fortran to calculate RDM for SQD and DQD (By the author)
6. Analytic continuation Fortran code to calculate MRS for SQD and DQD (Original codes by J. Thingna to calculate harmonic oscillator. Modified by the author to calculate SQD and DQD)

A short sample code for analytic NEGF calculation is given below

```
! This code is to calculate density matrix for single quantum dot follow DSH-
    PRE.85.011126
! By Xu Xiansong
! Last Updated: Wed Oct 28 09:14:24 SGT 2015
!-------------------------------------------------
    IMPLICIT NONE
    DOUBLE COMPLEX, ALLOCATABLE :: RHO0(:,:),RHO2(:,:)
    DOUBLE PRECISION :: E0,TL,TR,WD,G,uL,uR
    INTEGER :: I,J,L,N,IERR

    DOUBLE COMPLEX :: H,C1,C2,C3,C4,C5,C6,C7,C8,C9,C10,C11,P1,P2,SUMP3,P3,
        P3CHECK
    DOUBLE COMPLEX :: C12,C13,C14,P4,P4CHECK,SUMP4
    DOUBLE PRECISION, PARAMETER :: EPS=0.01D0, PREC=(10.0D0)**(-15.0D0),PI=
        ACOS(-1.0D0)
    DOUBLE PRECISION ::NUL1,NUL2
    DOUBLE COMPLEX :: d,a,checkn,D0,DCHECK
    DOUBLE COMPLEX,PARAMETER :: II=CMPLX(0.0D0,1.0D0)

    INTEGER :: COUNT1,COUNT2
    CHARACTER(LEN=15) :: E0_C,TL_C,TR_C,N_C,WD_C,G_C,UL_C,UR_C
!-------------Input Parameters---------------------------------
    CALL GET_COMMAND_ARGUMENT(1,E0_C)
    CALL GET_COMMAND_ARGUMENT(2,TL_C)
    CALL GET_COMMAND_ARGUMENT(3,TR_C)
    CALL GET_COMMAND_ARGUMENT(4,N_C)
    CALL GET_COMMAND_ARGUMENT(5,WD_C)
    CALL GET_COMMAND_ARGUMENT(6,G_C)
    CALL GET_COMMAND_ARGUMENT(7,UL_C)
    CALL GET_COMMAND_ARGUMENT(8,UR_C)
    READ (E0_C,*) E0
    READ (TL_C,*) TL
    READ (TR_C,*) TR
    READ (N_C,*) N
    READ (WD_C,*) WD
    READ (G_C,*) G
    READ (UL_C,*) UL
    READ (UR_C,*) UR
!-----------------------------------------------------------------
    ALLOCATE(RHO0(N,N),STAT=IERR)
    IF (IERR /= 0 ) WRITE(*,*) "Allocation␣Error␣for␣Rh0"
!------------------Calculate the integral d----------------------
!!-----------------First 3 poles (One of them is zero/The one on imaginary
    axis)--------------------------------
    H=SQRT(4.0D0*G*WD-(WD+II*E0)**2)
    C1=EXP(UL/TL+0.5d0/TR*(H+II*WD+E0))+EXP(UR/TR)*(2.0D0*EXP(UL/TL)+EXP(0.5D0
        /TL*(H+II*WD+E0)))
    C3=(4.0D0*II*G*WD-(WD+II*E0)*(H+II*WD-E0))
    C4=(EXP(UL/TL)+EXP(0.5D0/TL*(H+II*WD+E0)))*(EXP(UR/TR)+EXP(0.5D0/TR*(H+II*
        WD+E0)))
    P1=II*G*WD*C1/C3/C4

    C5=EXP(UL/TL+0.5D0/TR*(-H+II*WD+E0))+EXP(UR/TR)*(2.0D0*EXP(UL/TL)+EXP(0.5
        D0/TL*(-H+II*WD+E0)))
    C7=(4.0D0*G*WD+(E0-II*WD)*(H-II*WD+E0))
    C8=(EXP(UL/TL)+EXP(0.5D0/TL*(-H+II*WD+E0)))*(EXP(UR/TR)+EXP(0.5D0/TR*(-H+
        II*WD+E0)))
    P2=G*WD*C5/C7/C8
!-------------------Matsubara Sum-------------------------------
    P3=0.0D0
    P3CHECK=0.0D0
    COUNT1=0
    DO L=1,10000000
    NUL1=(L*2.0D0-1.0D0)*PI*TL
    C10=((G*WD-(UL-II*WD)*(UL-E0))+NUL1*(-2.0D0*II*UL-WD+II*E0)+NUL1**2)
    C11=((G*WD-(UL+II*WD)*(UL-E0))+NUL1*(-2.0D0*II*UL+WD+II*E0)+NUL1**2)

    P3=P3-TL*G*WD**2/C10/C11
    COUNT1=1+COUNT1
    IF (ABS(P3-P3CHECK) .GT. PREC) THEN
    P3CHECK=P3
    ELSE
    GOTO 10
    END IF
    END DO
10      SUMP3=P3*II
```

```
    P4=0.0D0
    P4CHECK=0.0D0
    COUNT2=0
    DO L=1,10000000
    NUL2=(L*2.0D0-1.0D0)*PI*TR
    C12=((G*WD-(UR-II*WD)*(UR-E0))+NUL2*(-2.0D0*II*UR-WD+II*E0)+NUL2**2)
    C13=((G*WD-(UR+II*WD)*(UR-E0))+NUL2*(-2.0D0*II*UR+WD+II*E0)+NUL2**2)

    P4=P4-TR*G*WD**2/C12/C13
    COUNT2=1+COUNT2
    IF (abs(P4-P4CHECK) .GT. PREC) THEN
    P4CHECK=P4
    ELSE
    GOTO 20
    END IF
    END DO
 20 SUMP4=P4*II
    D=P1+P2+SUMP3+SUMP4

!----------------------Output-----------------------------------
!   WRITE(*,*) "Count1",COUNT1
!   WRITE(*,*) "Count2",COUNT2
    WRITE(*,*) REAL(1.0D0-D)
!   WRITE(*,*) REAL(D)
!   WRITE(*,*) REAL((RHO0(1,1)))
!-------------Check for normalization-------------------------
!   CHECKN=RHO0(1,1)+RHO0(2,2)
!   WRITE(*,*) CHECKN
!-------------DSH RHO2 and higher order contribution----------
!   D0=1.0D0/(EXP((E0-UL)/TL)+1.0D0)+1.0D0/((EXP((E0-UR)/TR))+1.0D0)
!   D0=D0/2.0D0

!   WRITE(*,*) 'DSH RHO0',(1.0D0-D0)
!   WRITE(*,*) REAL((1.0d0-D)-(1.0d0-D0))
!   WRITE(*,*) REAL(D-D0)
    DEALLOCATE(RHO0)
END PROGRAM
```